

# Discovery of a Locally and Orally Active CXCL12 Neutraligand (LIT-927) with Anti-inflammatory Effect in a Murine Model of Allergic Airway Hypereosinophilia

Pierre Regenass,<sup>†,§</sup> Dayana Abboud,<sup>‡,§</sup> François Daubeuf,<sup>†,§,||</sup> Christine Lehalle,<sup>†,§,||</sup> Patrick Gizzi,<sup>||,§</sup> Stéphanie Riché,<sup>†,§</sup> Muriel Hachet-Haas,<sup>‡,§</sup> François Rohmer,<sup>†,§</sup> Vincent Gasparik,<sup>†,§</sup> Damien Boeglin,<sup>†,§</sup> Jacques Haiech,<sup>†,§</sup> Tim Knehans,<sup>†,§</sup> Didier Rognan,<sup>†,§</sup> Denis Heissler,<sup>†,§</sup> Claire Marsol,<sup>†,§,||</sup> Pascal Villa,<sup>||,§</sup> Jean-Luc Galzi,<sup>‡,§</sup> Marcel Hibert,<sup>†,§,||</sup> Nelly Frossard,<sup>\*,†,§</sup> and Dominique Bonnet<sup>\*,†,§,||</sup>

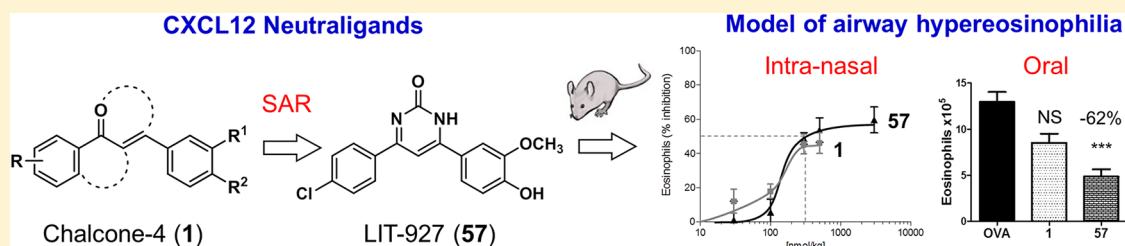
<sup>†</sup>Laboratoire d'Innovation Thérapeutique, Faculté de Pharmacie, UMR7200 CNRS/Université de Strasbourg, 74 route du Rhin, 67401 Illkirch, France

<sup>‡</sup>Biotechnologie et Signalisation Cellulaire, Ecole Supérieure de Biotechnologie de Strasbourg, UMR 7242 CNRS/Université de Strasbourg, Bld Sébastien Brant, 67412 Illkirch, France

<sup>||</sup>Plate-forme de chimie biologique intégrative de Strasbourg, UMS 3286 CNRS/Université de Strasbourg, 67412 Illkirch, France

<sup>§</sup>Labex MEDALIS, Université de Strasbourg, 67000 Strasbourg, France

## Supporting Information



**ABSTRACT:** We previously reported Chalcone-4 (1) that binds the chemokine CXCL12, not its cognate receptors CXCR4 or CXCR7, and neutralizes its biological activity. However, this neutraligand suffers from limitations such as poor chemical stability, solubility, and oral activity. Herein, we report on the discovery of pyrimidinone 57 (LIT-927), a novel neutraligand of CXCL12 which displays a higher solubility than 1 and is no longer a Michael acceptor. While both 1 and 57 reduce eosinophil recruitment in a murine model of allergic airway hypereosinophilia, 57 is the only one to display inhibitory activity following oral administration. Thereby, we here describe 57 as the first orally active CXCL12 neutraligand with anti-inflammatory properties. Combined with a high binding selectivity for CXCL12 over other chemokines, 57 represents a powerful pharmacological tool to investigate CXCL12 physiology in vivo and to explore the activity of chemokine neutralization in inflammatory and related diseases.

## INTRODUCTION

Chemokines are small proteins with critical roles in the development and function of various tissues in vertebrates.<sup>1–3</sup> As a rather general rule, chemokines and their G protein-coupled receptors display redundancy and binding promiscuity, i.e., one chemokine may bind to different receptors,<sup>4,5</sup> whereas chemokine receptors may be activated by various chemokines. A few chemokines play a pivotal and non-redundant homeostatic role, as is the case for CXCL12. In the adult, they regulate the directional migration of leukocytes under normal and pathological conditions.<sup>6</sup> They are associated with an extraordinary high number of diseases, including chronic inflammation,<sup>6</sup> autoimmune diseases (lupus erythematosus),<sup>7</sup> cancer,<sup>8,9</sup> atherosclerosis,<sup>10,11</sup> or AIDS;<sup>12</sup> their receptors have been considered as druggable targets.<sup>13</sup> Indeed, classical drug design strategies aim at discovering

chemokine receptor ligands, mainly antagonists, in order to regulate the associated functions.<sup>14,15</sup> Yet, many antagonists have disappointingly failed in clinical trials, which may be related either to chemokine receptor redundancy or to the difficulty of designing specific chemokine receptor antagonists.<sup>16,17</sup> We have recently opened a novel avenue for drug development in reporting a small molecule, “Chalcone-4” (1), that displays an original mechanism of action as it binds to the chemokine CXCL12, not to its two cognate receptors CXCR4 and CXCR7, and neutralizes its biological activity.<sup>18</sup> Chalcone-4 and related molecules have been termed “neutraligands” by analogy with neutralizing antibodies and proved to have therapeutic potential. Indeed, 1 inhibits binding of CXCL12 to

Received: April 25, 2018

Published: August 14, 2018

CXCR4 and CXCR7, reduces intracellular calcium responses, blocks chemotaxis of human peripheral blood CD4<sup>+</sup> lymphocytes, and prevents CXCR4 internalization in response to CXCL12.<sup>18</sup> This chemical compound is active in vivo in a mouse model of allergic airway eosinophilic inflammation, where it inhibits eosinophil infiltration in response to the allergen. It is also active in other disease models involving the CXCL12/CXCR4 axis such as the WHIM syndrome or carcinogenesis.<sup>19,20</sup> As the poor solubility of **1** prevented its local administration in the airways, we have previously successfully developed simple analogues of **1** acting as prodrugs to improve solubility and showed that a significant local bronchial activity was reached at a low dose.<sup>21</sup> We also developed an antedrug active when administered locally and inactivated when passing systemically, thereby preventing distant adverse events and thus optimizing the specificity of action.<sup>22</sup> Therefore, neutralizing CXCL12 by small compounds has proven to be a promising strategy to treat inflammatory diseases, in particular, asthma. However, all of these neutraligands encompass a chalcone chemotype and display major limitations including Michael acceptor character and poor oral activity. Very few other small organic compounds able to bind CXCL12 have been reported to date. Recently, in silico screening led to the identification of ZINC 310454,<sup>23</sup> obtained following a fragment-based structure–activity relationship (SAR) analysis,<sup>24</sup> with some activity on cell migration in vitro at micromolar concentrations. Other small molecule ligands have been identified for different binding sites on CXCL12, but neither in vitro nor in vivo activity has been reported yet.<sup>25</sup> Another example is the aptamer NOX-A12 that shows anti CXCL12 activity in vitro and in vivo but is not orally bioavailable.<sup>26</sup>

Here, we describe a systematic SAR study around **1** and the discovery of the first selective and orally active CXCL12 neutraligand **57** (LIT-927) derived from a pyrimidinone scaffold in an allergic airway eosinophilic inflammation in the mouse.

## RESULTS AND DISCUSSION

The physiological and pathophysiological importance of CXCL12 and CXCR4 has prompted us to launch drug discovery programs for various diseases. Chalcone-4 (**1**), previously identified following a high-throughput screening approach, binds to CXCL12, thereby preventing interaction with CXCR4.<sup>18</sup> However, **1** displays also some major drawbacks for drug development: (1) its solubility in aqueous media is low (9  $\mu$ M in PBS buffer); (2) the presence of the  $\alpha,\beta$ -unsaturated carbonyl group (often referred to as Michael acceptor) allows 1,4-additions with thiols;<sup>27</sup> (3) it is not active in vivo in murine models of allergic airway hypereosinophilia by the oral route.

To overcome these limitations, **1** was selected as the starting point for further structural optimization. The modular nature of this compound made it particularly well suited for utilization of array synthesis to efficiently explore the SAR of the chemotype. Optimization efforts went along four directions: (i) exploration of the substitution on ring A, (ii) exploration of the substitution on ring B, (iii) modification of the central core (CC) of **1**, and (iv) design of rigid isosteres (Figure 1).

**Synthesis.** Chalcones **2–31** were prepared from an acetophenone and a benzaldehyde by a Claisen–Schmidt reaction using barium hydroxide hydrate as a base.<sup>28</sup> When necessary, methoxymethyl (MOM) deprotection was carried

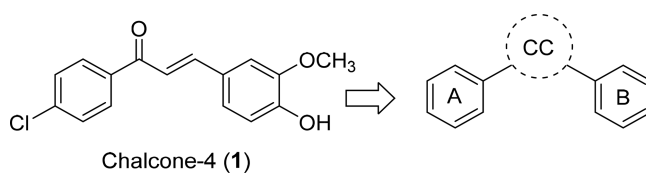


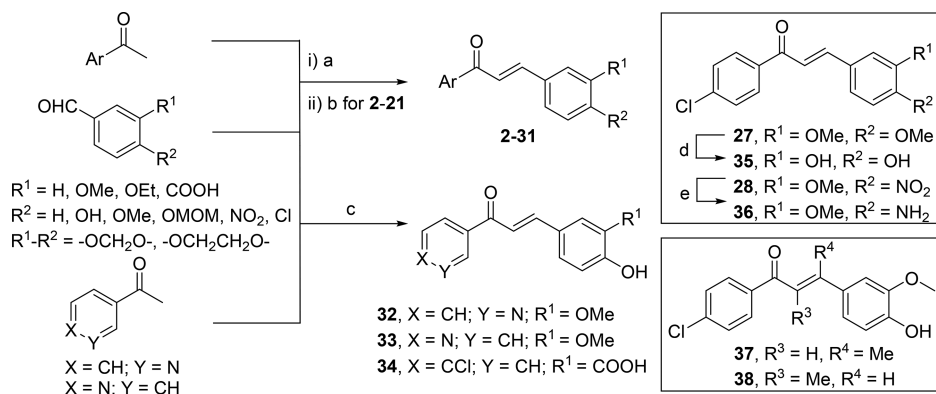
Figure 1. SAR strategy around Chalcone-4 (**1**).

out with concentrated hydrochloric acid in THF (Scheme 1). In some cases, the condensation was advantageously performed under acidic conditions by bubbling hydrogen chloride through a dichloromethane solution of the reagents (**32** and **33**) or using a mixture of aqueous hydrogen chloride and sulfuric acid (**34**). Interestingly, compound **1** was best synthesized by carefully adding thionyl chloride to an ethanolic solution of the two carbonyl partners, thus generating hydrogen chloride in situ. In some cases, additional steps were required. Thus, amino derivative **36** was prepared by reduction of the corresponding nitro precursor **28** in the presence of iron in acidic ethanol, whereas **35** was obtained by demethylation of the methoxy substituents with boron tribromide in dichloromethane. Chalcone **37** was prepared from 1-(4-chlorophenyl)but-2-yn-1-one and (4-bromo-2-methoxyphenoxy) (*tert*-butyl)dimethylsilane using *n*-butyllithium and copper(I) bromide, followed by deprotection of TBDMS with sodium hydroxide. Chalcone **38** was obtained by treatment of the corresponding carbonyl compounds with pyridinium acetate/piperidine.

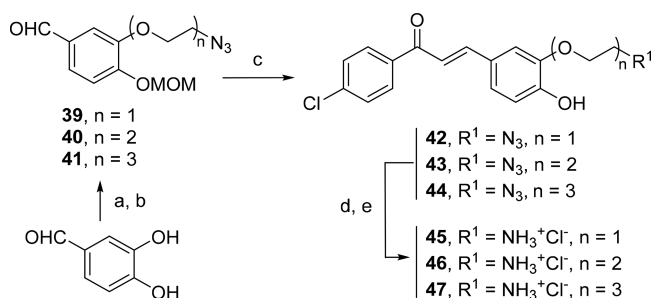
In order to increase water solubility of the target compounds, we planned to introduce a hydrophilic chain on ring B. Scheme 2 describes the synthesis of these modified chalcones. Treatment of 3,4-dihydroxybenzaldehyde in the presence of an excess of sodium hydride to deprotonate both hydroxyl groups and of an azido sulfonate led to alkylation at the more reactive 3-phenate site. Subsequent protection of the 4-hydroxyl moiety as a methoxymethyl ether gave compounds **39–41** that were condensed with *p*-chloroacetophenone as previously described.<sup>28</sup> Finally, MOM deprotection followed by Staudinger reduction of azides **42–44** in THF–water enabled access to **45–47** as their hydrochloride salts.

Several other analogues were prepared from **1** as shown in Scheme 3. Thus, 1,3-diarylpropan-1-one **48** was obtained by hydrogenation on platinum(IV) oxide and oxime **49** by reaction with hydroxylamine. Treatment with hydrazine hydrate in ethanol afforded the pyrazoline **50** or its *N*-acetyl analogue **51** when acetic acid was added to the reaction, both compounds being obtained as racemic mixtures. Several pyrimidines could be obtained by condensation of **1** either with imidamides (**52–54**), guanidines (**55** and **56**), or urea (**57**). The pyrazole **60** could be prepared by hydrazine hydrate treatment and MOM deprotection of diketone **59** prepared from 4-chloroacetophenone and MOM-protected methyl vanillate **58**.

Constrained chalcones, incorporating an additional 5- or 6-membered ring, were also synthesized by reacting 6-chloro-3(2*H*)-benzofuranone, 6-chlorotetral-1-one, and 7-chlorochroman-4-one with 4-hydroxy-3-methoxybenzaldehyde under the conditions already mentioned in Scheme 1. Due to the poor solubility of **61** in aqueous media, 6-chlorobenzofuran-1-one was reacted with benzaldehyde **40** bearing a hydrophilic ethylene glycol chain to provide after Staudinger reduction the more soluble compound **63**. Better solubility may also be obtained if the additional ring is an oxygenated heterocycle.

Scheme 1. Synthesis of Compounds 1–38<sup>a</sup>

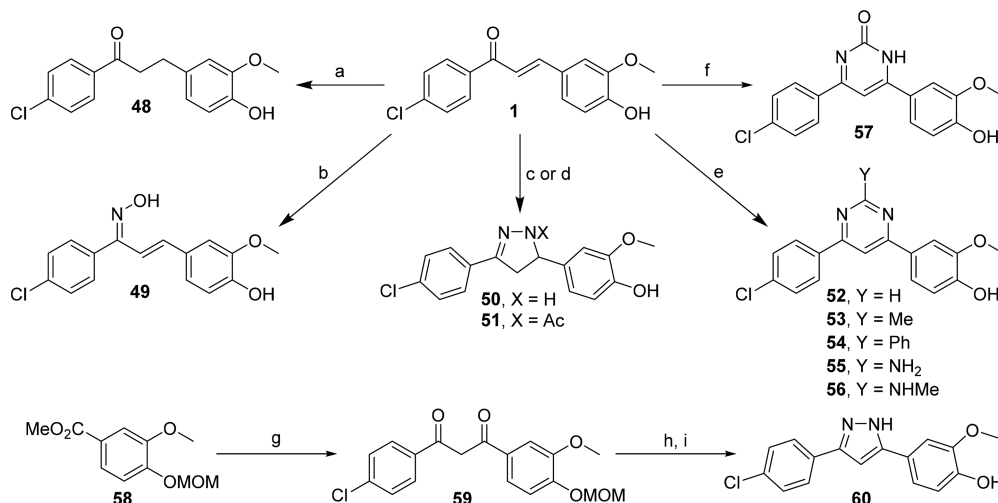
<sup>a</sup>Reagents and conditions: (a)  $\text{Ba}(\text{OH})_2 \cdot \text{H}_2\text{O}$ ,  $\text{EtOH}$ , rt, 20 h, 19–97%. For preparation of **14**  $\text{NaOH}$ ,  $\text{EtOH}$ , 80 °C, 16 h, 38%. **15**:  $\text{KOH}$ ,  $\text{EtOH}/\text{H}_2\text{O}$  (1/1), rt, 16 h, 95%. (b) Aqueous  $\text{HCl}$ ,  $\text{THF}$ , rt, 16 h, 53–100%. (c) **32** and **33**:  $\text{HCl}$ ,  $\text{MeOH}$ , rt, 2 h, 12–30%. **34**: aqueous  $\text{HCl}$ ,  $\text{H}_2\text{SO}_4$ , rt, 16 h,  $\text{DMF}$ , 2%. (d)  $\text{BBr}_3$ ,  $\text{CH}_2\text{Cl}_2$ , 0 °C to rt, 16 h, 10%. (e)  $\text{Fe}$ , aqueous  $\text{HCl}$ ,  $\text{EtOH}$ , 80 °C, 2 h, 25%

Scheme 2. Synthesis of Chalcones with Increased Water Solubility<sup>a</sup>

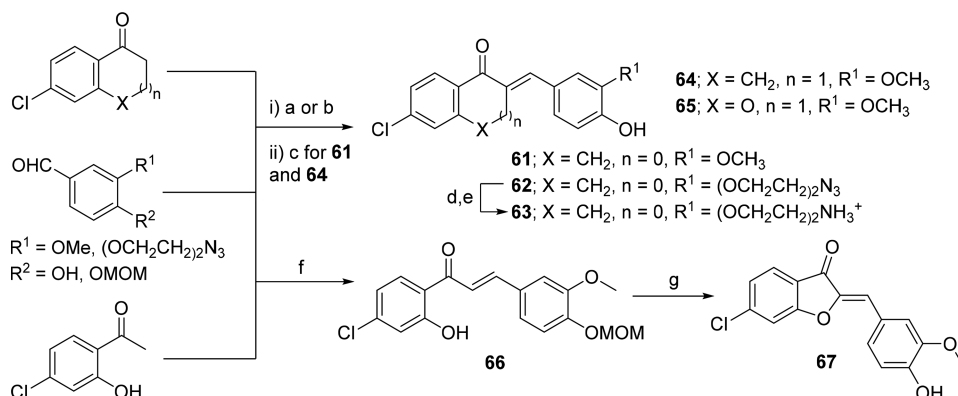
<sup>a</sup>Reagents and conditions: (a)  $\text{NaH}$ ,  $\text{DMSO}$ ,  $\text{Ts}(\text{OCH}_2\text{CH}_2)_n\text{N}_3$  for **39** and **40** or  $\text{Ms}(\text{OCH}_2\text{CH}_2)_3\text{N}_3$  for **41**, 0 °C, 1 h, then rt, 16 h, 68–76%. (b)  $\text{MOMCl}$ ,  $\text{K}_2\text{CO}_3$ , acetone, rt, 16 h, 95–100%. (c) 4- $\text{Cl-C}_6\text{H}_4\text{C}(\text{O})\text{Me}$ ,  $\text{Ba}(\text{OH})_2 \cdot \text{H}_2\text{O}$ ,  $\text{EtOH}$ , rt, 4 h, 30–56%. (d) 12 M  $\text{HCl}$ ,  $\text{THF}$ , rt, 16 h, 100%. (e)  $\text{PS-PPh}_3$  for **45** and **46** or  $\text{TCEP-HCl}$  for **47**,  $\text{THF}/\text{H}_2\text{O}$ , rt, 16 h, 50–70%

We therefore prepared the benzofuran-3-one **67** by treating **66** with mercury(II) acetate in anhydrous pyridine (Scheme 4). All compounds were fully characterized by  $^1\text{H}$  and  $^{13}\text{C}$  NMR and MS analysis and were obtained with a purity > 95%.

**Structure–Activity Relationship and Structural Optimization.** Pharmacomodulation of **1**, the first small organic compound-based chemokine neutraligand, led to a structure–activity relationship analyzed in a systematic way by studying the consequences on CXCL12 binding of structural modifications of the 4-chloro aromatic ring (ring A; Table 1), of the phenolic part (ring B; Table 2), and of the central core of **1** (Table 3). Finally, rigid isosteres were prepared and tested to characterize the active conformation of **1** and to potentially improve its affinity and bioavailability (Table 4). The ability of each novel compound to inhibit CXCL12–CXCR4 interactions was carefully evaluated by using FRET-based binding experiments as previously described.<sup>18,29,30</sup> In this assay, binding of Texas red-labeled CXCL12 (CXCL12-TR) to CXCR4 fused to EGFP expressed at HEK293 cell

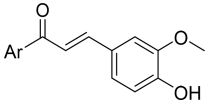
Scheme 3. Synthesis of Compound 1 Derivatives with Central Core Modifications<sup>a</sup>

<sup>a</sup>Reagents and conditions: (a)  $\text{PtO}_2$ ,  $\text{H}_2$ ,  $\text{EtOAc}$ , rt, 20 min, 46%. (b)  $\text{NH}_2\text{OH}$ , pyridine, rt, 16 h, 43%. (c)  $\text{NH}_2\text{NH}_2 \cdot \text{H}_2\text{O}$ ,  $\text{EtOH}$ , 80 °C, 4 h, 47%. (d)  $\text{NH}_2\text{NH}_2 \cdot \text{H}_2\text{O}$ ,  $\text{AcOH}$ ,  $\text{EtOH}$ , 80 °C, 18 h, 69%. (e)  $\text{H}_2\text{N-CY=NH}$  ( $Y = \text{H, Me, Ph, NH}_2, \text{NHMe}$ ),  $\text{DMF}$ , base, 20–53%. (f) urea,  $\text{HCl}$ , dioxane/ $\text{EtOH}$ , 100 °C, 2 h, 43%. (g)  $\text{NaH}$ , 4- $\text{Cl-C}_6\text{H}_4\text{C}(\text{O})\text{Me}$ ,  $\text{THF}$ , 0 °C, 1 h, 70 °C, 16 h, 32%. (h)  $\text{NH}_2\text{NH}_2 \cdot \text{H}_2\text{O}$ ,  $\text{EtOH}$ , 80 °C, 10 h, 84%. (i) 12 M  $\text{HCl}$ ,  $\text{THF}$ , rt, 16 h, quant.

Scheme 4. Synthesis of Conformationally Constrained Analogues<sup>a</sup>

<sup>a</sup>Reagents and conditions: (a) Ba(OH)<sub>2</sub>·H<sub>2</sub>O, MeOH/EtOH, rt, 16 h, 28–48%. (b) SOCl<sub>2</sub>, EtOH, 53–100%. (c) 12 M HCl, THF, rt, 16 h, quant. (d) PS–PPh<sub>3</sub>, THF/H<sub>2</sub>O (4/1), 70 °C, 4 h, 20%. (e) 1 M HCl, rt, 30 min, quant. (f) Ba(OH)<sub>2</sub>·H<sub>2</sub>O, EtOH, rt, 48 h, 28%. (g) Hg(AcO)<sub>2</sub>, pyridine, 110 °C, 2 h, 25%

**Table 1.** Effect of the Substituents of Ring A on CXCL12-TR Binding

|  |       |                                |  |  |
|---|-------|--------------------------------|--|--|
| entry   | compd | solubility, <sup>a</sup><br>μM | Ar   | inhibition of CXCL12-<br>TR binding, K <sub>i</sub> [nM] |
| 1   | 1     | >5                             | 4-Cl-C <sub>6</sub> H <sub>4</sub> –                 | 53 ± 31  |
| 2   | 2     | >5                             | 2-Cl-C <sub>6</sub> H <sub>4</sub> –                 | 107 ± 35   |
| 3   | 3     | >5                             | 3-Cl-C <sub>6</sub> H <sub>4</sub> –                 | 25% of inhibition at<br>30 μM <sup>b</sup>               |
| 4   | 4     | >5                             | 4-F-C <sub>6</sub> H <sub>4</sub> –                  | 430 ± 214  |
| 5   | 5     | >5                             | 4-Br-C <sub>6</sub> H <sub>4</sub> –                 | 44 ± 17  |
| 6   | 6     | >5                             | 4-I-C <sub>6</sub> H <sub>4</sub> –                  | 107 ± 17   |
| 7   | 7     | >5                             | Ph–  | >10 000  |
| 8   | 8     | >5                             | 4-Me-C <sub>6</sub> H <sub>4</sub> –                 | 285 ± 17   |
| 9   | 9     | >5                             | 4-CF <sub>3</sub> -C <sub>6</sub> H <sub>4</sub> –   | 1070 ± 230   |
| 10  | 10    | 1.92                           | 4- <i>i</i> -Pr-C <sub>6</sub> H <sub>4</sub> –      | 25 ± 10  |
| 11  | 11    | 0.95                           | 2-naphthyl–  | 5% of inhibition at<br>30 μM <sup>b</sup>                |
| 12  | 12    | >5                             | 4-MeO-C <sub>6</sub> H <sub>4</sub> –                | 1780 ± 714   |
| 13  | 13    | >5                             | 4-NO <sub>2</sub> -C <sub>6</sub> H <sub>4</sub> –   | 30% of inhibition at<br>30 μM <sup>b</sup>               |
| 14  | 14    | >5                             | 4-HO <sub>2</sub> C-C <sub>6</sub> H <sub>4</sub> –  | 5350 ± 750   |
| 15  | 15    | >5                             | 4-HSO <sub>3</sub> -C <sub>6</sub> H <sub>4</sub> –  | 6% of inhibition at<br>30 μM <sup>b</sup>                |
| 16  | 16    | >5                             | 2-F-4-Cl-C <sub>6</sub> H <sub>3</sub> –             | 107 ± 11   |
| 17  | 17    | >5                             | 2,3-Cl <sub>2</sub> -C <sub>6</sub> H <sub>3</sub> – | 357 ± 20   |
| 18  | 18    | >5                             | 2,4-Cl <sub>2</sub> -C <sub>6</sub> H <sub>3</sub> – | 48 ± 17  |
| 19  | 19    | >5                             | 2,5-Cl <sub>2</sub> -C <sub>6</sub> H <sub>3</sub> – | 53 ± 11  |
| 20  | 20    | >5                             | 2,6-Cl <sub>2</sub> -C <sub>6</sub> H <sub>3</sub> – | 71 ± 21  |
| 21  | 21    | >5                             | 3,4-Cl <sub>2</sub> -C <sub>6</sub> H <sub>3</sub> – | 714 ± 285  |
| 22  | 32    | >5                             | 3-Py–  | >10 000  |
| 23  | 33    | >5                             | 4-Py–  | >10 000  |

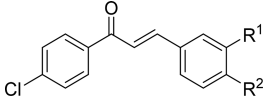
<sup>a</sup>Solubility of compounds in HEPES-BSA buffer. <sup>b</sup>Limited by the solubility of the compound in HEPES-BSA buffer.

membrane induces fluorescence resonance energy transfer (FRET) between the EGFP and the Texas red, which can be monitored by the reduction of EGFP fluorescence emission at 510 nm. This reduction of EGFP fluorescence is dose dependently inhibited by molecules that bind either CXCR4 or CXCL12 in a competitive manner.

**Influence of Ring A Substitution on CXCL12 Binding.** The potency of series 1 analogues obtained by ring A modification to inhibit CXCL12-TR binding to the EGFP-tagged CXCR4 receptor (K<sub>i</sub>) are listed in Table 1. The solubility of all compounds at a 5 μM concentration was validated before binding assessment. Interestingly, the unsubstituted phenyl derivative 7 is completely inactive at 10 μM (entry 7), indicating that the chalcone chemotype is not sufficient on its own for binding the chemokine, as already reported.<sup>18</sup> Substitution at position 4 with halogens results in a dramatic increase in affinity with an optimum observed for chlorine (1) and bromine (5) with K<sub>i</sub> = 53 and 44 nM, respectively (entries 1 and 5). A 2-fold decrease is observed with iodine (6), while a 4-fluoro substituent displays a 10-fold decrease in affinity (4) (entries 6 and 4). Chlorine and bromine may represent the best compromise in terms of size, electronegativity, and polarizability. The influence of position 4 substituents was further explored with limited success. Hence, methylation (8) provides a neutral ligand with a K<sub>i</sub> = 430 nM, whereas its electron-withdrawing trifluoromethyl isostere 9 is even less potent (K<sub>i</sub> = 1 070 nM) with an affinity comparable to the electron-donating 4-methoxy derivative 12 (K<sub>i</sub> = 1 780 nM) (entries 8, 9, and 12). Interestingly, the hydrophobic and bulky 4-isopropyl group (10) further improves the potency down to K<sub>i</sub> = 25 nM (entry 10). However, its limited water solubility renders difficult its further in vivo evaluation. Finally, a series of three compounds with electron-withdrawing substituents in position 4 was tested (13, 14, and 15). None of them shows a significant affinity for CXCL12 or CXCR4 (entries 13, 14, and 15). In summary, the chloro, bromo, and isopropyl substituents display the highest affinities, suggesting that bulkiness and polarizability are more important structural determinants of activity than electron-withdrawing or electron-donating properties. The 3-chlorophenyl analogue 3 shows a drastically reduced potency, while the 2-chloro isostere 2 retains a good affinity (K<sub>i</sub> = 107 nM) with only a 2-fold decrease compared to 1. The detrimental role of the 3-chloro substitution is confirmed with the disubstituted compounds 17 and 21: the 3,4-dichloro derivative 17 is indeed 14-fold less potent than 11, while the 2,4-dichloro analogue 18 is equipotent (K<sub>i</sub> = 48 nM) (entries 17, 11, and 18). The 2-fluoro-4-chloro compound 16 also retains a significant potency (K<sub>i</sub> = 107 nM) (entry 16). Similarly, if one compares the



Table 2. Effect of the Substituents of Ring B on CXCL12-TR Binding



| entry | compd | R <sup>1</sup>   | R <sup>2</sup>   | solubility, <sup>a</sup> $\mu$ M | inhibition of CXCL12-TR binding, K <sub>i</sub> (nM) |
|-------|-------|--|------------------|----------------------------------|--|
| 1     | 1     | -OMe   | -OH              | >5                               | 53 $\pm$ 31  |
| 2     | 22    | -OH  | -OMe             | >5                               | >10 000  |
| 3     | 23    | -H   | -H               | 1.17                             | 18% of inhibition at 1 $\mu$ M <sup>b</sup>          |
| 4     | 24    | -OCH <sub>2</sub> O-   |                  | 2.31                             | 25% of inhibition at 3 $\mu$ M <sup>b</sup>          |
| 5     | 25    | -OCH <sub>2</sub> CH <sub>2</sub> O-   |                  | >5                               | 1380 $\pm$ 357                                       |
| 6     | 26    | -OMe   | -H               | 0.36                             | >10 000  |
| 7     | 27    | -OMe   | -OMe             | >5                               | >10 000  |
| 8     | 28    | -OMe   | -NO <sub>2</sub> | >5                               | >10 000  |
| 9     | 29    | -H   | -OH              | >5                               | 625 $\pm$ 3  |
| 10    | 30    | -OEt   | -OH              | 4.72                             | 52% of inhibition at 5 $\mu$ M <sup>b</sup>          |
| 11    | 34    | -CO <sub>2</sub> H   | -OH              | >5                               | >10 000  |
| 12    | 35    | -OH  | -OH              | >5                               | 350 $\pm$ 85   |
| 13    | 36    | -OMe   | -NH <sub>2</sub> | >5                               | >10 000  |
| 14    | 45    | -OCH <sub>2</sub> CH <sub>2</sub> NH <sub>3</sub> <sup>+</sup> Cl <sup>-</sup>                 | -OH              | >5                               | 357 $\pm$ 121  |
| 15    | 46    | -(OCH <sub>2</sub> CH <sub>2</sub> ) <sub>2</sub> NH <sub>3</sub> <sup>+</sup> Cl <sup>-</sup> | -OH              | >5                               | 1071 $\pm$ 321                                       |
| 16    | 47    | -(OCH <sub>2</sub> CH <sub>2</sub> ) <sub>3</sub> NH <sub>3</sub> <sup>+</sup> Cl <sup>-</sup> | -OH              | >5                               | 475 $\pm$ 71   |

<sup>a</sup>Solubility max of compound in HEPES-BSA buffer. <sup>b</sup>Limited by the solubility of the compound in HEPES-BSA buffer.

potency of the 2-chloro derivatives with a second chlorine in positions 3, 5, and 6 (17, 19, and 20, respectively), one observes the worst potency when a chlorine is in position 3 and an affinity comparable to 1 for the 2,5-dichloro analogue 19 ( $K_i$  = 53 nM) (entries 17, 19, and 20). Noteworthy, the replacement of the phenyl moiety by a naphthyl (11) or a 3- or 4-pyridinyl (32 and 33) failed to provide active compounds (entries 11, 22, and 23).

**Influence of Ring B Substitution on CXCL12 Binding.** In order to study the contribution of substitutions on ring B (Table 2), a series of analogues with a 4-chlorophenyl as ring A was synthesized. The water solubility of these analogues and their potency to inhibit the chemokine binding are listed in Table 2. Two ring B substituents are present in the original hit 1: a methoxy group in position 3 and a hydroxyl in position 4. The derivative 23 with an unsubstituted aromatic ring B is only weakly active and has a low solubility in water (entry 2). When the methoxy group on ring B is absent (22), a 10-fold decrease in affinity is observed (entry 2), whereas a loss of affinity occurs when only the methoxy group is preserved (26) (entry 6). These findings suggest that the 4-hydroxy is more important than the 3-methoxy for the affinity toward CXCL12. When the hydroxyl and methoxy groups of 1 are inverted as in 22, no activity is detected (entry 2). Compound 35 with a 3,4-dihydroxyphenyl ring B is almost two times more active than 29 bearing only a 4-hydroxyl group (entries 12 and 9). These results indicate that the presence and the position of the methoxy and hydroxyl substituents on ring B are crucial and contribute greatly to the affinity of compounds to CXCL12. Furthermore, when the hydroxyl group of 1 is replaced by a methoxy (27), a nitro (28), or an amino group (36), the activity is very low (entries 7, 8, and 12). Accordingly, the cyclic dioxo analogues 24 and 25 are almost inactive (entries 4 and 5). These results clearly demonstrate the crucial role of the hydroxyl group at the 4 position on ring B.

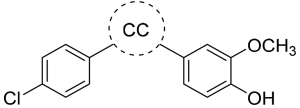
In contrast, the nature of the R<sup>1</sup> alkoxy group can be fine tuned without a drastic loss of affinity (30) (entry 10). Thus, a

2-(polyethoxy)ethan-1-aminium hydrophilic side chain was introduced at this position to improve the solubility properties, the best results being obtained with compounds 45 and 47 (entries 14 and 16).

**Influence of Central Part Substitution and Stiffening.** Having determined the most suitable substituents on rings A and B, we next examined the influence of the central part of 1 on the affinity for CXCL12 (Tables 3 and 4). The reduction of the olefinic bond leads to the inactive compound 48 (Table 3, entry 4), likely due to the modification of both the electron distribution and the conformation of the molecule. The oxime 49, the chalcone 31 where ring A and ring B have switched position, or 37 and 38 with a trisubstituted double bond have no significant activity on CXCL12 binding ( $K_i$  > 5  $\mu$ M) (Table 3, entries 1, 2, 3, and 5). In our hands only the  $\alpha$ -cyano derivative (CN-Chalcone 4, Figure 2) retains a good activity ( $K_i$  = 53 nM). This compound was previously reported active in vivo, behaving as an antedrug with potential therapeutic application.<sup>29</sup>

We then attempted to rigidify the central oxopropenyl moiety of 1 in two ways: (1) by building a 5- or 6-membered heterocycle on this oxopropenyl connector (Table 3); (2) by bridging the ortho position of ring A with C-2 of the oxopropenyl linker by one or two atoms (Table 4). In the first series, the pyrazoline 50 is particularly interesting since it retains a good affinity ( $K_i$  = 107 nM) and shows that the  $\alpha,\beta$ -unsaturated ketone moiety is not mandatory in this case, compared to 48 (entries 4 and 6). The acetylated derivative 51 however has a drastically reduced activity (entry 7). Surprisingly enough, the pyrazole 60 is an inactive analogue, though the conjugated system has been restored, thus showing the subtlety of the docking of these molecules (entry 14). Conjugated six-membered ring analogues, pyrimidines 52–56, have a poor activity (entries 8 and 12). The simplest, unsubstituted pyrimidine 52 shows a very modest inhibition (30%) at 5  $\mu$ M (entry 8). The activity is slightly improved by substitution with a methyl (53), showing the possibility to reach a hydrophobic pocket (entry 9). However, substitution

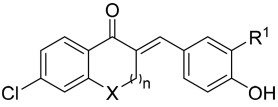
Table 3. Effect of Modification of Central Core (CC) on CXCL12-TR Binding



| Entry | Compd     | Central core | Solubility <sup>a</sup> , $\mu\text{M}$ | Inhibition of CXCL12-TR binding, $K_i$ (nM)         |
|-------|-----------|--------------|---|---|
| 1     | <b>31</b> |              | >5                                      | > 10 000  |
| 2     | <b>37</b> |              | 2.6                                     | > 10 000  |
| 3     | <b>38</b> |              | >5                                      | > 5 000   |
| 4     | <b>48</b> |              | nd                                      | > 10 000  |
| 5     | <b>49</b> |              | >5                                      | > 10 000  |
| 6     | <b>50</b> |              | >5                                      | 107 $\pm$ 71  |
| 7     | <b>51</b> |              | >5                                      | > 10 000  |
| 8     | <b>52</b> |              | 4.29                                    | 30% of inhibition at 5 $\mu\text{M}$ <sup>b</sup>   |
| 9     | <b>53</b> |              | >5                                      | 1 680 $\pm$ 71                                      |
| 10    | <b>54</b> |              | 0.53                                    | 20% of inhibition at 0.3 $\mu\text{M}$ <sup>b</sup> |
| 11    | <b>55</b> |              | >5                                      | > 10 000  |
| 12    | <b>56</b> |              | >5                                      | > 10 000  |
| 13    | <b>57</b> |              | >5                                      | 267 $\pm$ 71  |
| 14    | <b>60</b> |              | 19.5                                    | > 10 000  |

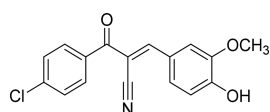
<sup>a</sup>Solubility of compounds in HEPES-BSA buffer. <sup>b</sup>Limited by the solubility of the compound in HEPES-BSA buffer.

Table 4. Effect of Stiffening by Forming a 5- or 6-Membered Ring Fused with Ring A on CXCL12-TR Binding



| entry | compd     | X                  | n | R <sup>1</sup>   | solubility, <sup>a</sup> $\mu\text{M}$ | inhibition of CXCL12-TR binding, $K_i$ (nM)        |
|-------|-----------|--------------------|---|--|--|--|
| 1     | <b>61</b> | —CH <sub>2</sub> — | 0 | —OMe   | 0.88                                   | 107 $\pm$ 2  |
| 2     | <b>63</b> | —CH <sub>2</sub> — | 0 | —(OCH <sub>2</sub> ) <sub>2</sub> NH <sub>3</sub> <sup>+</sup> Cl <sup>−</sup> | >5                                     | 496 $\pm$ 285                                      |
| 3     | <b>64</b> | —CH <sub>2</sub> — | 1 | —OMe   | >5                                     | 70% of inhibition at 10 $\mu\text{M}$ <sup>*</sup> |
| 4     | <b>65</b> | —O—                | 1 | —OMe   | >5                                     | 357 $\pm$ 114                                      |
| 5     | <b>67</b> | —O—                | 0 | —OMe   | >5                                     | 203 $\pm$ 71                                       |

<sup>a</sup>Solubility of compounds in HEPES-BSA buffer.

Figure 2. Structure of the  $\alpha$ -cyano derivative of CN-Chalcone 4.

by a phenyl group (**54**) or by the more polar amino groups (**55**, **56**) erases the activity (entries 10–12). In contrast, the oxo analogue **57** retains a very significant activity ( $K_i = 267$  nM) though 5-fold lower than **1** (entry 13). Noteworthy, **57** presents a more rigid core than **1** that freezes the central chain in the all-trans conformation, indicating that this corresponds to the active conformation of **1**. It is in agreement with crystal structures of both **1** and **57** that are very well superimposable

(Supporting Information, Figure S1 and Tables S1 and S2). Interestingly, the pyrimidinone nucleus in structure **57** is different from the overexploited chalcone chemotype. Furthermore, it contains more heteroatoms than **1**, which results in an increased water solubility (36 versus 9  $\mu\text{M}$ ; Table 5, entry 5). As a consequence, **57** represents an interesting lead compound that was studied in vivo as detailed below.

**Table 5. Solubility and Stability of Selected Neutraligands**

| entry | compd     | solubility, <sup>a</sup> $\mu\text{M}$ |         | stability, <sup>b</sup> % |         |
|-------|-----------|--|---------|---------------------------|---------|
|       |           | PBS                                    | PBS/Cdx | PBS                       | PBS/Cdx |
| 1     | <b>1</b>  | 9                                      | >300    | 100                       | 100     |
| 2     | <b>6</b>  | 1.2                                    | 319     | 100                       | 100     |
| 3     | <b>45</b> | 4.2                                    | >5000   | 100                       | 100     |
| 4     | <b>50</b> | 34.6                                   | >3000   | 78                        | 98      |
| 5     | <b>57</b> | 36.4                                   | >5000   | 100                       | 100     |
| 6     | <b>65</b> | 0.5                                    | 933     | 100                       | 100     |
| 7     | <b>67</b> | 1.9                                    | 330     | 100                       | 100     |

<sup>a</sup>Measured at pH 7.4 in PBS or PBS/Cdx, 24 h of incubation, 22 °C.

<sup>b</sup>Percentage of remaining compound monitored by RP-HPLC after 24 h at 37 °C.

The second series of rigidified compounds proved to be interesting as well (Table 4). Linking ring A with the  $\alpha,\beta$ -unsaturated ketone via a methylene bridge as in benzofuranone **61** halves the activity ( $K_i = 107$  nM) relative to **1** (entry 1). This 2-fold decrease in affinity might stem from a higher hydrophobicity. Bridging with two methylene units as in tetralone **64** (entry 3) leads to a very low activity that may result from a less favorable conformation or from an excessive hydrophobicity. An oxy bridge leads to **67**, which is slightly less active than **61** ( $K_i = 203$  nM) but has a better water solubility (>5  $\mu\text{M}$  vs 0.88  $\mu\text{M}$ ; entries 1 and 5), whereas the oxymethylene derivative **65** is another less potent but still active compound ( $K_i = 357$  nM; solubility > 5  $\mu\text{M}$ ; entry 4). In summary, two out of three rotatable bonds of the central core of compound **1** can be incorporated into rigid systems while retaining the ability to inhibit CXCL12 binding to its CXCR4 receptor in the nanomolar range. This supports the idea that the active conformation of **1** is probably very close to its conformation in its crystal structure. However, very subtle changes in the structure may lead to a dramatic loss of activity, suggesting that this series of ligands interacts with a well-defined and stringent binding site. At this point it was necessary to demonstrate that these derivatives of molecule **1** are indeed neutraligands, that is, that they interfere with CXCL12-CXCR4 binding in actually binding to the chemokine and not to its receptor.

**Neutraligand Characterization.** For the most potent compounds **6**, **45**, **50**, **57**, **65**, and **67** arising from the above SAR studies, confirmation of their neutralizing properties was achieved using the procedure previously described (Figure 3).<sup>31</sup> Briefly, using the FRET-based binding assay, the characterization of CXCL12 neutraligands was evaluated in two conditions, differing by the sequence of addition of the molecules. Hence, reduction of EGFP fluorescence emission is more pronounced when neutraligands are preincubated (30 min) with the cells expressing CXCR4 receptor than when preincubated with CXCL12 prior to the addition to the cells, indicating that preliminary binding to the chemokine is the mechanism of action, and the compounds are neutraligands and not receptor antagonists. Following this procedure data

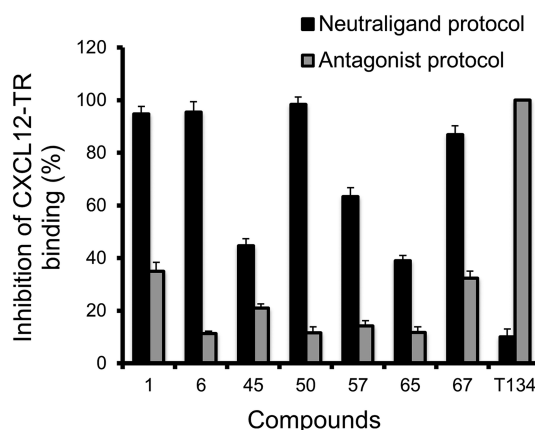


**Figure 3.** Inhibition of CXCL12-TR binding when neutraligands are incubated with the CXCR4-EGFP-fused receptor-expressing cells prior to addition of CXCL12 (black bars; neutraligand protocol) or with CXCL12 prior to addition to CXCR4-EGFP-fused receptor-expressing cells (gray bars; antagonist protocol). Compounds were tested at a concentration of  $10 \times K_i$  (inhibition constant). CXCR4 antagonist T134 (20  $\mu\text{M}$ ) was used as a control in both incubation protocols. Each column represents the mean (block)  $\pm$  SD (bars) of  $n = 3$  experiments.

obtained for all six compounds are consistent with a binding to the chemokine and not to the receptor (Figure 3). Consequently, all selected compounds are indeed CXCL12 chemokine neutraligands and behave as **1**.

**In Vivo Evaluation of New Neutraligands.** The six compounds identified as CXCL12 neutraligands were selected for in vivo studies. The iodo analogue **6** is slightly less potent than **1** in vitro ( $K_i = 107$  vs 53 nM, respectively) but was selected since it may represent a valuable imaging probe for in vivo pharmacokinetic studies by single-photon-emission-computed tomography once  $I^{123}$  radiolabeled. Compound **45** is a direct derivative of **1** branched with a water-solubilizing side chain. Compounds **50**, **57**, **65**, and **67** are the most potent and soluble cyclic neutraligands identified in vitro and are representative of four novel chemotypes: pyrazoline, pyrimidinone, benzofuranone, and chromanone. First, their solubility in assay media was evaluated (Table 5). (2-Hydroxypropyl)- $\beta$ -cyclodextrin (Cdx) was used as the excipient because of its low toxicity and capacity to increase the bioavailability of chemical compounds.<sup>32</sup> Solubility studies in PBS/Cdx (10% w/w) showed that all compounds are soluble at least at a 300  $\mu\text{M}$  concentration (Table 5). The compound stability was evaluated in PBS or in PBS/Cdx. Only **50** was unstable in PBS, but the degradation could be avoided when Cdx was added (entry 4). Next, the in vivo activity of the selected compounds was evaluated in the 8-day murine model of allergic airway eosinophilic inflammation previously described (Figure 4A).<sup>21,33</sup> Briefly, Balb/c mice were sensitized to ovalbumin (OVA) in the presence of alum and challenged 3 times at 24 h intervals with OVA in saline or saline alone. Treatment with each compound (300 nmol/kg in 10% PBS/Cdx) was administered by the intranasal route 2 h before each challenge. A bronchoalveolar lavage was performed 24 h after the last challenge and inflammatory cell number quantified.<sup>34</sup>

Interestingly, despite a low solubility, the iodo-chalcone **6** retained a very good in vivo activity since it reduced eosinophil infiltration by 36% while the hit compound **1** reduced it by 47% at the same dose. Compounds **45**, **65**, and **67** were almost

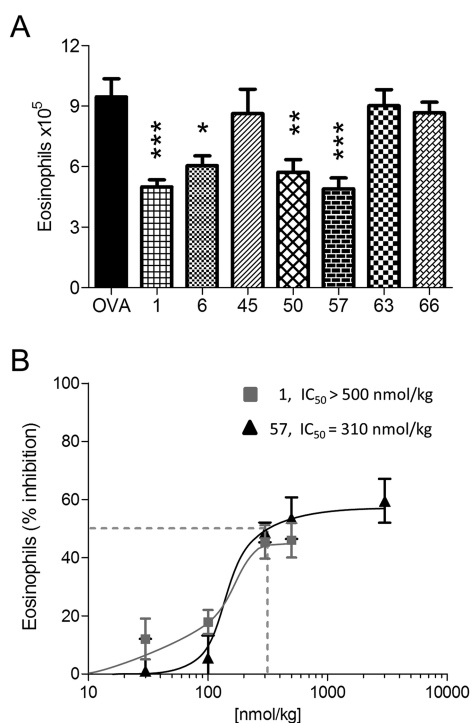


**Figure 4.** In vivo anti-inflammatory activity of CXCL12 neutraligands administered topically (i.n.) in the 8-day mouse model of allergic airway hypereosinophilia. (A) Topical treatment with compounds **1**, **6**, **45**, **50**, **57**, **65**, and **67** (300 nmol/kg) in PBS/CdX 10% (vehicle) administered 2 h before each allergen challenge. Absolute numbers of eosinophils, neutrophils, and lymphocytes in bronchoalveolar lavage fluid (BAL) are shown. Blocks are means, and error bars are SEM values ( $n = 6/\text{group}$ ). Statistical analysis has been protected by a Bonferroni test.  $^{\#}P \leq 0.05$  and  $^{\#\#\#}P \leq 0.001$  vs vehicle-treated saline group and  $*P \leq 0.05$ ,  $**P \leq 0.01$ ;  $***P \leq 0.001$  vs vehicle-treated OVA group. (B) Dose–response effect of topical treatment with compounds **1** and **57** (i.n.). Compounds **1** (gray line) and **57** (black line) solubilized in PBS/CdX 10% were administered 2 h before each allergen challenge. Percentage of inhibition of eosinophil recruitment in the bronchoalveolar lavage is shown. Data points are means, and bars are SEM values ( $n = 6/\text{group}$ ).

inactive in our assay and were not further investigated. More interestingly, the two other rigidified analogues **50** and **57** that had similar in vitro potency displayed very good to excellent in vivo activity, inhibiting eosinophil infiltration by 39% and 48%, respectively (Figure 4A). Noteworthy, the recruitment of macrophages and lymphocytes was not affected by treatment with the CXCL12 neutraligands in this model when neutrophil numbers were reduced with a trend toward significance (not shown). The chemical instability of **50** observed during both synthesis and storage precluded the separation of both isomers and their further in vitro and in vivo evaluation. We therefore decided to select **57** as lead neutraligand and characterized its activity ( $\text{IC}_{50}$ ) in vivo in a dose–response efficacy study versus **1** on eosinophil recruitment in our mouse model. The  $\text{IC}_{50}$  of the reference compound **1** could not be determined precisely because the solubility threshold was reached at 500 nmol/kg even when solubilized in PBS/Cdx. In contrast, the soluble novel pyrimidinone **57** gave an  $\text{IC}_{50}$  calculated as 310 nmol/kg (Figure 4B).

We thereafter characterized further (1) the Michael-acceptor reactivity of **57**, (2) its binding properties to CXCL12, and (3) its selectivity toward other chemokines.

**Michael-Acceptor Reactivity.** The Michael-acceptor character of **57** and **1** was evaluated in the presence of glutathione (GSH, 2.5 equiv). As determined by LC-MS analysis, after 2 h at 37 °C, more than 30% of **1** was converted into the GSH-**1** adduct while **57** was found to be much more stable without any formation of GSH-**57** adduct (Supporting Information, Figure S2).

**Biophysical Characterization.** To support the neutraligand character of **57** reported above from FRET-based binding assay, the binding to CXCL12 was examined by monitoring changes in its emission of tryptophan fluorescence intensity (Figure 6). Indeed, as previously reported, CXCL12 contains a single tryptophan residue (Trp-57) whose intrinsic fluorescence can be modulated by neutraligands.<sup>18</sup> Thus, we observed that tryptophan fluorescence intensity at 340 nm (excitation at 285 nm) declined monotonically when CXCL12 (2  $\mu\text{M}$ ) was incubated with increasing concentrations of **57** (Figure 6C). The resulting tryptophan fluorescence inhibition curve was satisfactorily fitted according to a 1:1 stoichiometry interaction mode, and the deduced dissociation constant ( $K_d = 780 \pm 320$  nM) was in the same range as that determined by FRET-based assay ( $K_i = 267 \pm 71$  nM).

As a control from the whole strategy, the structurally close pyrimidinone **68** (Figure 5A) was synthesized (Supporting Information for the synthesis) and tested in the FRET-based assay described above (Figure 5B). Thereby, **68** inhibited CXCL12 binding to CXCR4 by less than 5% at 300  $\mu\text{M}$ . In the tryptophan fluorescence assay, **68** nonspecifically decreased Trp fluorescence intensity at 340 nm (Figure 5C). Additionally, **68** was inactive in the mouse model of allergic airway eosinophilic inflammation at 300 nmol/kg (data not shown).

**Molecular Modeling of Compounds **1** and **57** Bound to CXCL12.** Physicochemical properties as well as the herein presented structure–activity relationship suggest a common binding mode of compounds **1** and **57** to CXCL12 that completely differs from that observed with the inhibitor recently described.<sup>24</sup> The later compound is bound to a wide and accessible pocket, which is incompatible with the observed nanomolar binding affinities of our neutraligands. We therefore envisaged the possibility of an alternative and mostly apolar pocket that would be just large enough to tightly host compound **1** or **57**. Systematic scanning of the CXCL12 chemokine dimeric structure<sup>24</sup> with the in-house developed VolSite program<sup>35</sup> clearly indicates the presence of a small but structurally druggable pocket (Figure 6A) at the vicinity of Trp57, whose importance to compound **1** binding has previously been evidenced by fluorescence spectroscopy.<sup>18</sup> Docking of compounds **1** and **57** to this pocket is possible at the condition to allow side-chain flexibility for three residues (Arg20, Trp57, and Tyr61, Figure 6) that would control the entry to the Trp57 pocket. Two independent docking algorithms, Plants<sup>36</sup> and Surflex-Dock,<sup>37</sup> agree to similarly dock both compounds in a manner that is almost fully consistent with the herein described structure–activity relationships, assuming a common binding mode for compounds **1** and **57** (Figure 6B and 6C). First, the 4-chlorophenyl ring A is deeply buried in an apolar subpocket (Val23, Leu26, Trp57) whose size is nicely complementary to that of a 4-chlorophenyl substituent. The observed lower affinity of the 3-chlorophenyl analog **3** can be easily explained by close proximity of Leu26 or Trp57 backbone atoms that would prevent a complete entry into the pocket. Second, the proposed binding mode also explains the crucial role of a 4-



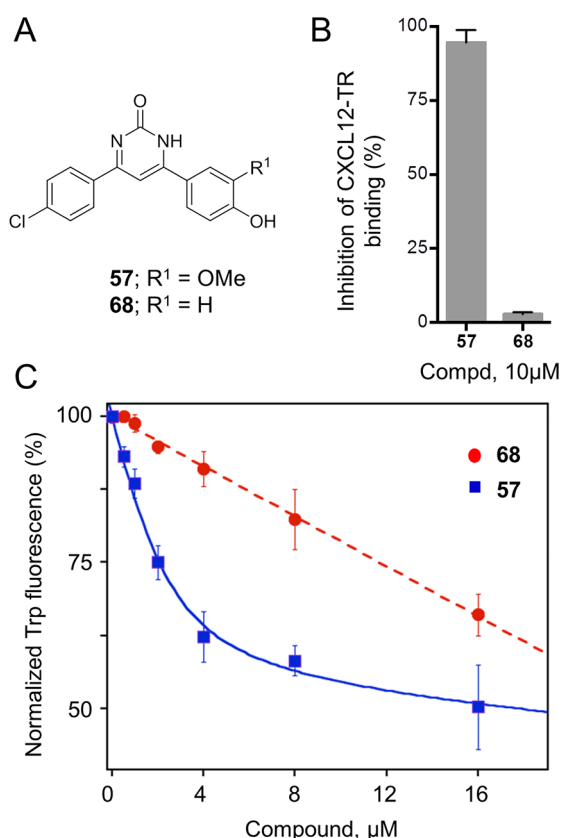


**Figure 5.** Interaction between 57 and CXCL12. (A) Chemical structure of pyrimidinone 68 as compared to 57. (B) Inhibition of CXCL12-TR binding when 57 and 68 (10 μM) are incubated with the CXCL12 chemokine prior to addition to CXCR4-EGFP fused receptor-expressing cells. (C) Titration of binding of pyrimidinones 57 (squares) and 68 (circle) to CXCL12 determined by monitoring changes in the maximal emission of Trp fluorescence of CXCL12 (measured at 340 nm). Increasing amounts of molecule were added to CXCL12 solution (2 μM in Hepes buffer). Equation used to fit experimental data is the root of the second-order equation:  $(RL)^2 + (RL) \times (-Ro - Lo - K_D) + Ro \times Lo = 0$  where  $(RL) = ((Ro + Lo + K_D) \pm ((-Ro - Lo - K_D)^2 - 4 \times Ro \times Lo)^{1/2})/2$  and where Ro, the concentration of chemokine, is set to 2 μM, Lo is the initial concentration of molecule,  $K_D$  is the dissociation constant of a molecule for the chemokine, and RL is the fractional concentration of the receptor and ligand complex. Data are means (dots) and SD (bars) values of three independent experiments.

hydroxyphenyl ring B. The aromatic ring is stacked between Pro32 and the ammonium moiety of Lys64 to which a  $\pi$ -cation interaction is observed in our model. The hydroxyl group in ring B donates a hydrogen bond to the nearby Gln37 side chain, thereby explaining the higher affinity of the hydroxyle with respect to the methoxy analog. Third, the ketone moiety of compound 1 is hydrogen bonded to Arg20 side chain (Figure 6C). In the case of compound 57, the bioisosteric pyrimidin-2(1H)-one core is ideally located to accept a bidentate hydrogen bond from Arg20 side chain (Figure 6B). Contrary to compound 57, compound 1 is predicted to adopt another possible binding mode (Figure 6D) in which positions of aromatic rings A and B had been interchanged, the ketone being still anchored to Arg20. Depending on the substituents at rings A and B, the binding mode may readily switch from one to the other possible orientations.

In the proposed binding mode, the absolute binding free energy of compounds 1 (preferred binding mode) and 57, computed by the Hyde scoring function,<sup>38</sup> is estimated to be  $-18.60$  and  $-14.92$  kJ mol<sup>-1</sup>, close to the experimentally observed values of  $-17.78$  and  $-16.06$  kJ mol<sup>-1</sup>, respectively.

**Binding Selectivity toward Other Chemokines.** The selectivity of 57 was evaluated toward four other chemokines, namely, CCL17, CCL22, CCL5, and CCL2, by using the neutraligand protocol of the recently reported time-resolved intracellular calcium recording (TRIC-r) assay<sup>39</sup> (Figure 7). This generic assay enables the discovery of chemokine-neutralizing molecules (neutraligands) by differentiating them from molecules that block the receptor (antagonists). Initially described for the identification of CCL17 and CCL22 neutraligands, the assay has been setup for CXCL12.<sup>39</sup> Thereby, as depicted in Figure 7, pyrimidinone 57 at 10 μM is able to inhibit the increase in intracellular calcium concentration in EGFP-CXCR4<sup>+</sup> HEK cells in response to CXCL12, while it has no effect on calcium responses triggered by either CCL17 or CCL22 on EGFP-CCR4<sup>+</sup> HEK cells, CCL5 on EGFP-CCR5<sup>+</sup> HEK cells, or CCL2 on EGFP-CCR2<sup>+</sup> HEK cells. These results demonstrate the high selectivity of 57 toward CXCL12 vs other chemokines also involved in asthma.

**In Vivo Evaluation of Neutraligand 57 Activity and Safety.** At this stage of the study pyrimidinone 57 turned out to be a CXCL12-selective neutraligand with markedly improved solubility and no longer Michael acceptor character. In addition, we demonstrated its anti-inflammatory activity at low dose after local administration in a murine model of allergic airway hypereosinophilia. These results prompted us to further evaluate 57 in vivo. We first compared the activity and safety of compounds 1 and 57 versus the main commercialized comparators, the CXCR4 antagonist AMD3100 and the glucocorticoid dexamethasone (Dex) in the mouse model of hypereosinophilia. The compounds were administered i.p. 2 h before the allergen challenge. Neutraligands 1 and 57 (350 μmol/kg) inhibited eosinophil infiltration by 54% and 55% and AMD3100 (12.6 μmol/kg) and Dex (2.5 μmol/kg) by 33% and 59%, respectively (Figure 8A). The anti-inflammatory activity of AMD3100 and Dex was accompanied by a statistically reliable decrease in body and spleen weight, indicating major adverse event-related perturbation by these compounds. In contrast, neutraligands 1 and 57 did not exhibit any side effects (Figure 8B). Even after 10 daily administrations of neutraligands 1 or 57, no weight loss was observed (Figure 8B) or other signs of toxicity, prostration, bristly hair (not shown), which ascertains that our two neutraligands are safe. This result was confirmed by the absence of a lesion in our Gomori's staining histological studies of liver, spleen, heart, and kidney (Supporting Information Figure S3). In addition, our experiment shows the antiasthma activity of the CXCR4 antagonist AMD3100 in our model of allergic airway hypereosinophilia in a same potency as reported in a model of cockroach-induced asthma.<sup>40</sup> Altogether these results confirm that the prevention of the interaction between CXCL12 and CXCR4 axis by our CXCL12 neutraligands could be a beneficial and safe strategy for asthma treatment. Finally, we evaluated the oral activity of our novel neutraligand 57, which could be an interesting additional approach for asthma treatment. We investigated the oral activity of the CXCL12 neutraligands 1 and 57 administered by gavage (1400 μmol/kg) as assessed in the same murine model of

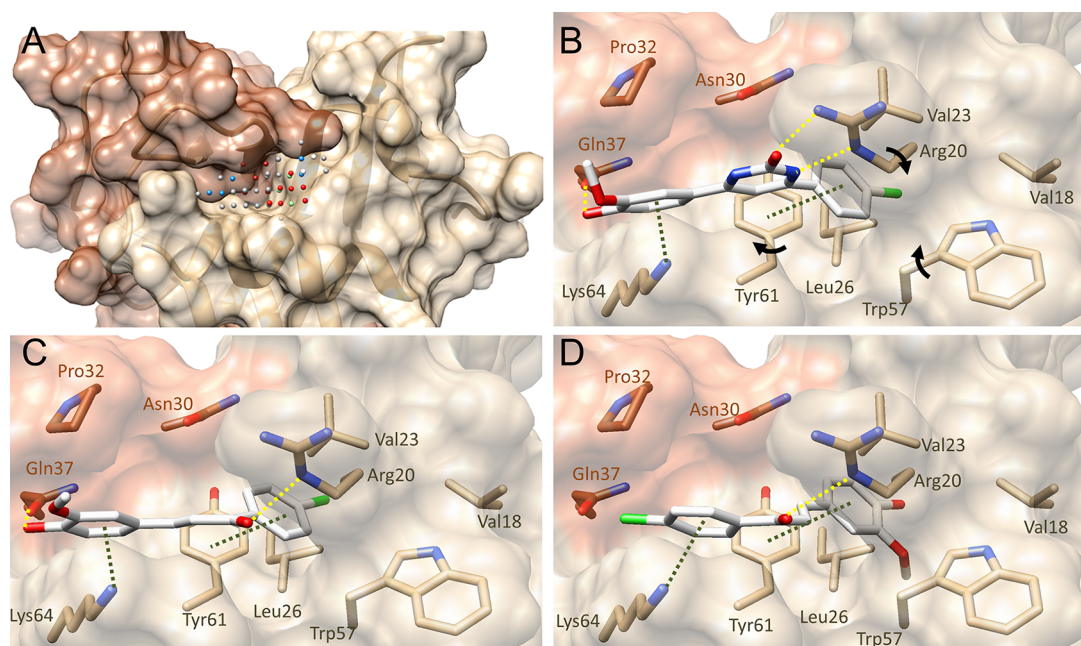


**Figure 6.** Hypothesized binding mode of compounds **1** and **57** to the CXCL12 homodimer. Two monomers are displayed by a transparent surface and backbone ribbons (monomer 1, tan; monomer 2, sienna). (A) Detection of a druggable cavity (colored spheres) nearby Trp57 at the surface of the CXCL12 homodimer (PDB ID 4UAI). Volume of the cavity, detected by VolSite,<sup>35</sup> is 184 Å<sup>3</sup>. Cavity points are colored by pharmacophoric properties (red, hydrogen-bond acceptor; blue, hydrogen-bond donor; gray, hydrophobic/aromatic). (B) PLANTS docking pose of compound **57** to CXCL12. Three side chains (indicated by an arrow) are allowed to freely move, thereby widening the pocket volume up to 371 Å<sup>3</sup>. Hydrogen bonds are indicated by yellow broken lines. Aromatic and  $\pi$ -cation interactions are represented by dark green broken lines. Residues contributing to the binding cavity are labeled at their C- $\alpha$  atom (tan, monomer 1; sienna, monomer 2). (C) PLANTS preferred docking pose of compound **1** to CXCL12. (D) PLANTS alternative docking pose of compound **1** to CXCL12.

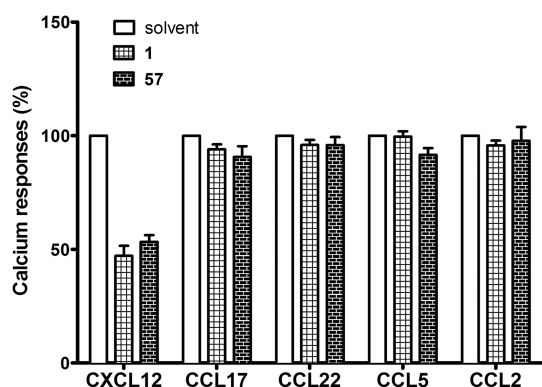


**Figure 7.** Selectivity of compounds **1** and **57** toward 5 chemokines. Effect of DMSO (white bars) and compound **1** or **57** (10  $\mu$ M) on calcium responses triggered by either 5 nM CXCL12 on EGFP-CXCR4<sup>+</sup> HEK cells, by 5 nM CCL17 and CCL22 on EGFP-CCR4<sup>+</sup> HEK cells, 5 nM CCL5 on EGFP-CCR5<sup>+</sup> HEK cells, or by 5 nM CCL2 on EGFP-CCR2<sup>+</sup> HEK cells. Each column represents the mean (block)  $\pm$  SD (bars) of  $n = 3$  experiments.

hypereosinophilia (Figure 8C). Neutraligand **57** shows a large and statistically reliable inhibition of eosinophil recruitment (62% inhibition), whereas compound **1** only exhibited a trend toward inhibition. Therefore, **57** is reported as the first orally active CXCL12 neutraligand in this model of asthma.

## CONCLUSION

We and others previously demonstrated that it is possible to identify small nonpeptidic molecules able to bind chemokines and prevent their binding to chemokine receptors, thus neutralizing their function.<sup>18,21,22,35</sup> Such molecules were

termed neutraligands due to their ability to neutralize a ligand, the chemokine, and to prevent interaction with its target receptor. We already reported CXCL12 neutraligands administered as prodrugs<sup>21</sup> or antedrug neutraligands<sup>22</sup> with in vivo potential at inhibiting airway eosinophilic inflammation. However, these compounds display major drawbacks for drug development such as owning a Michael acceptor-type scaffold limiting its potential in drug development. To overcome these limitations, we explored herein the structure–activity relationship around the first CXCL12 neutraligand **1**.<sup>18</sup> Pharmacomodulation opportunities on the three parts of the molecule were explored. 4-Chloro or 4-isopropyl are the most potent substituents on the acylated phenyl ring of the chalcone backbone. Interestingly, the iodo analogue compound **6** retained in vitro and in vivo activity that might be exploited in the future for radioimaging studies. We also identified that the 3-methoxy-4-hydroxy combination pattern remained the most efficient one on the other phenyl ring of the chalcone motif with very little freedom for pharmacomodulation. The central core of the molecule is very sensitive to any structural change. Interestingly, it was possible to move away from the chalcone backbone by rigidifying the flexible and thiol-reactive  $\alpha,\beta$ -unsaturated ketone by incorporation in cyclic systems. Thereby, a pyrazoline and a pyrimidinone derivatives were found to behave as novel CXCL12 neutraligands with affinities in the 100 nM range in vitro and a significant in vivo activity in a model of allergic eosinophilic airway inflammation. To summarize, pyrimidinone **57** is a valuable analog of **1** for further in vivo studies of CXCL12 implication in in vitro and in vivo models. Its slightly reduced intrinsic affinity for CXCL12 is largely compensated for by enhanced chemical and biological stabilities and physicochemical properties that

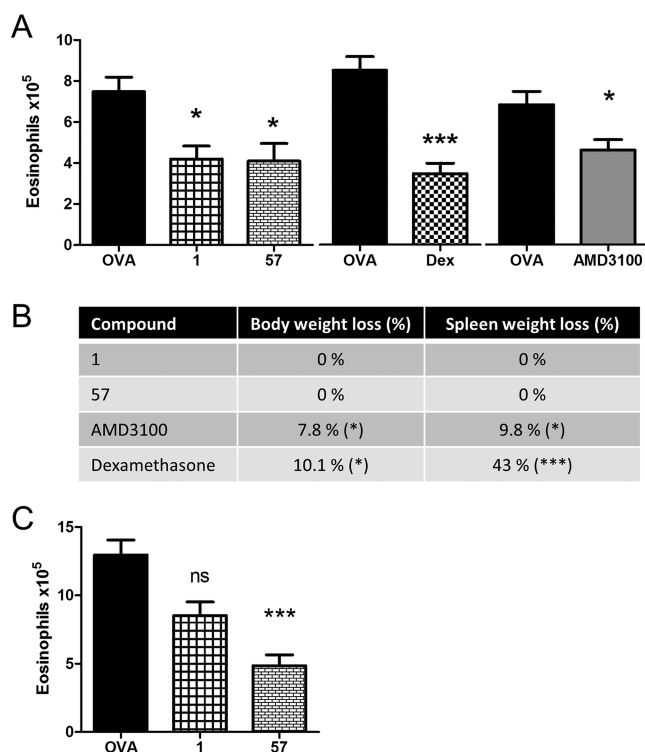


**Figure 8.** Anti-inflammatory activity of CXCL12 neutraligands in a mouse model of allergic eosinophilic airway inflammation. (A) Effect of systemic (i.p.) treatment with compounds **1** and **57** compared to the glucocorticoid dexamethasone (Dex) and the CXCR4 antagonist AMD3100 (Plerixafor) in the 8-day mouse model of allergic airway hyper-eosinophilia. Neutraligands **1** and **57** (350  $\mu\text{mol/kg}$  in PBS/CMC 1%), dexamethasone (2.5  $\mu\text{mol/kg}$ ), or AMD3100 (12.6  $\mu\text{mol/kg}$ ) were administered intraperitoneally 2 h before each challenge. Absolute numbers of eosinophils in BAL fluid are shown. Blocks are means, and error bars are SEM values ( $n = 6/\text{group}$ ). (B) Side effects of treatment with compounds **1** and **57** compared to Dex and AMD3100 measured on body and spleen weight loss in the model here above (24 h after three daily administrations). (C) Effect of oral treatment with compounds **1** and **57** in the 8-day mouse model of hyper-eosinophilia. Compounds in PBS/CMC 0.5%/Tween 80 0.05% (1400  $\mu\text{mol/kg}$ ) were administered intraperitoneally 2 h before each allergen challenge. Absolute numbers of eosinophils in BAL fluid are shown. Blocks are means, and error bars are SEM values ( $n = 6/\text{group}$ ). Statistical analysis has been protected by a Bonferroni test. \* $P \leq 0.05$ , \*\*\* $P \leq 0.001$  in comparison with vehicle-treated OVA group. Thereby, pyrimidinone **57** herein reported is a novel neutraligand able to bind selectively CXCL12 and to inhibit CXCL12–CXCR4 interaction. As compared to hit compound **1**, pyrimidinone **57** displays an improved solubility and chemical stability. Finally, neutraligand **57** inhibits allergic eosinophilic airway inflammation in mice when administered orally or locally.

allow improved in vivo potency in the murine model of hyper-eosinophilia. In particular, **57** is no longer a Michael acceptor. This therefore allows one to rule out covalent labeling of CXCL12 as the mechanism of action of **1** and its chalcone-derived analogs. In addition, **57** is more soluble and therefore more potent at reducing eosinophil recruitment, which is attained at very low doses after i.n. administration ( $\text{IC}_{50} = 300 \text{ nmol/kg}$ , i.e. 100  $\mu\text{g/kg}$ ) in the murine model of allergic eosinophilic asthma. In addition, **57** is the first orally active CXCL12 neutraligand, exhibiting anti-inflammatory activity when administered per os. Altogether, these results demonstrate that **57** represents a stable, selective, locally, and

orally active pharmacological tool to investigate the physiological and pathophysiological functions associated with the CXCL12–CXCR4 axis and a first step on the route toward the development of anti-inflammatory and novel antiasthma drugs.

## EXPERIMENTAL PROCEDURES

**Material and Methods. Chemistry.** Reagents were obtained from commercial sources and used without any further purification. Thin-layer chromatography was performed on silica gel 60F<sub>254</sub> plates. Flash chromatography was performed on silica gel cartridges (SiliaSep Flash cartridges silica, 40–63  $\mu\text{m}$ ) or RP18 prepacked columns (PuriFlash 30  $\mu\text{m}$ , Interchim) using a Spot II Ultimate apparatus from Armen Instrument. Semipreparative RP-HPLC were performed on one of the following columns: SunFire C18 OBD (5  $\mu\text{m}$ , 19  $\times$  150 mm, Waters) or SymmetryShield RP 18 (7  $\mu\text{m}$ , 19  $\times$  300 mm, Waters) on PLC2020 from Gilson using MeCN–0.1% TFA/water–0.1% TFA gradient (flow rate 15 mL/min) unless otherwise specified.

$^1\text{H}$  and  $^{13}\text{C}$  NMR spectra were recorded on Bruker 400 MHz/100 MHz, 300 MHz/75 MHz, and 200 MHz/50 MHz spectrometers. Conditions are specified for each spectrum (temperature 25  $^\circ\text{C}$  unless specified). Chemical shifts are reported in parts per million (ppm) relative to residual solvent, and coupling constants ( $J$ ) are reported in Hertz (Hz). Signals are described as s (singlet), d (doublet), t (triplet), q (quartet), m (multiplet), dd (doublet of doublets), dt (doublet of triplets), dq (doublet of quadruplets), and br s (broad singlet).

Analytical HPLC analyses were performed on an Agilent 1000 series apparatus equipped with an Ascentis Express C18 column (2.7  $\mu\text{m}$ , 4.6  $\times$  7.5 mm) under the following conditions: flow rate 1.6 mL/min; buffer A 0.1% aqueous TFA, buffer B 0.1% TFA in  $\text{CH}_3\text{CN}$ ; 5–95% buffer B over 7 min; detection  $\lambda = 220/254 \text{ nm}$ . For each compound, HPLC purity was  $\geq 95\%$ . LC/MS spectra were obtained on an Agilent HPLC single-quadrupole spectrometer (1200RR/LC/1956b-SL) equipped with a THERMO Hypersyl column (1.9  $\mu\text{m}$ , 1  $\times$  30 mm) using an Agilent Multimode ion source. HRMS spectra were obtained on an Accurate-Mass Q-TOF spectrometer from Agilent using electrospray ionization (ESI). Infrared (IR) spectra were recorded in inverse wavenumbers ( $\text{cm}^{-1}$ ) on a Thermo Nicolet 380 FT-IR spectrometer. The melting points of the solid compounds were measured with a Büchi B-540.

**Chalcone Synthesis under Basic Conditions—General Procedure A.** To a solution of the desired substituted benzaldehyde (2.00 mmol, 1.0 equiv) and acetophenone (2.00 mmol, 1.0 equiv) derivative in EtOH (5 mL) was added  $\text{Ba}(\text{OH})_2 \cdot \text{H}_2\text{O}$  (4.00 mmol, 2.0 equiv). The reaction was stirred at rt. After completion of the reaction, the mixture was evaporated under reduced pressure. Water was added to the residue, and the mixture was extracted three times with EtOAc or  $\text{CH}_2\text{Cl}_2$ . The combined organic layers were dried over anhydrous sodium  $\text{Na}_2\text{SO}_4$ , filtered, and concentrated. Purification on a silica gel column or semipreparative HPLC afforded the desired product.

**Methoxymethylation of Phenol—General Procedure B.** To a solution of a phenol derivative (1.50 mmol, 1.0 equiv) in anhydrous MeCN or DMF (2 mL) were added  $\text{K}_2\text{CO}_3$  (3.00 mmol, 2.0 equiv) and methoxymethyl chloride (2.25 mmol, 1.5 equiv). The mixture was stirred overnight at rt. After removal of the solvent under reduced pressure, water was added to the residue and the aqueous layer was extracted 3 times with EtOAc or  $\text{CH}_2\text{Cl}_2$ . The combined organic layers were dried over anhydrous  $\text{Na}_2\text{SO}_4$ , filtered, and concentrated to afford the desired compound without purification.

**Deprotection of Methoxymethyl Ether—General Procedure C.** To a solution of a methoxymethyl ether derivative (1.00 mmol) in THF (5 mL) was added concentrated aqueous HCl (8 drops). The mixture was allowed to stir overnight at rt and then evaporated to afford the desired compound. Purification on a silica gel column or by semipreparative RP-HPLC was performed if necessary.

**(E)-1-(4-Chlorophenyl)-3-(4-hydroxy-3-methoxyphenyl)prop-2-en-1-one (**1**).** To a solution of 4-hydroxy-3-methoxybenzaldehyde (4.92 g, 32.3 mmol) and 1-(4-chlorophenyl)ethan-1-one (5.0 g, 32.3 mmol) in EtOH (16 mL) at 0  $^\circ\text{C}$  was slowly added  $\text{SOCl}_2$  (1.65 mL,



22.7 mmol). The mixture was allowed to warm to rt and was stirred overnight. Water was added to the solution, and the mixture was extracted 2 times with  $\text{CH}_2\text{Cl}_2$ . The combined organic layers were dried over anhydrous  $\text{Na}_2\text{SO}_4$ , filtered, and concentrated. The solid was recrystallized from EtOH to give a yellow solid (7.37 g, 25.5 mmol, 79%).  $^1\text{H}$  NMR (400 MHz,  $\text{MeOD}-d_4$ )  $\delta$  8.05 (d,  $J$  = 8.6 Hz, 2H), 7.74 (d,  $J$  = 15.5 Hz, 1H), 7.56 (d,  $J$  = 15.5 Hz, 1H), 7.52 (d,  $J$  = 8.6 Hz, 2H), 7.35 (d,  $J$  = 2.0 Hz, 1H), 7.21 (dd,  $J$  = 8.2 Hz,  $J$  = 2.0 Hz, 1H), 7.17 (d,  $J$  = 1.9 Hz, 1H), 6.84 (d,  $J$  = 8.2 Hz, 1H), 3.93 (s, 3H);  $^{13}\text{C}$  NMR (100 MHz,  $\text{CDCl}_3$ )  $\delta$  191.2, 151.6, 149.6, 147.8, 140.2 (2C), 138.4, 131.3, 130.1, 128.3, 125.4, 119.5, 116.8 (2C), 112.4, 56.7; HRMS (ESI-TOF) calcd for  $\text{C}_{16}\text{H}_{14}\text{ClO}_3$  [ $\text{M} + \text{H}$ ] $^+$  289.06260, found 289.06356; mp 113–115  $^\circ\text{C}$ ; IR (Neat) 3505, 1650, 1577, 1509, 1432, 1272, 1215, 1158, 1027, 979, 817, 505, 474  $\text{cm}^{-1}$ .

**(E)-3-(4-Hydroxy-3-methoxyphenyl)-1-(4-iodophenyl)prop-2-en-1-one (6).** General procedure A, from 1-(4-iodophenyl)ethan-1-one (251 mg, 1.02 mmol) and 3-methoxy-4-(methoxymethoxy)benzaldehyde (200 mg, 1.02 mmol), 46% yield, then general procedure C, quantitative yield.  $^1\text{H}$  NMR (400 MHz,  $\text{CDCl}_3$ )  $\delta$  9.73 (br s, 1H), 7.93 (ABq, 4H,  $\Delta\delta_{\text{AB}}$  = 0.05,  $J_{\text{AB}}$  = 8.6 Hz), 7.70 (ABq, 2H,  $\Delta\delta_{\text{AB}}$  = 0.03,  $J_{\text{AB}}$  = 15.3 Hz), 7.51 (d,  $J$  = 2.0 Hz, 1H), 7.28 (dd,  $J$  = 8.3, 2.0 Hz, 1H), 6.83 (d,  $J$  = 8.3 Hz, 1H), 3.87 (s, 3H);  $^{13}\text{C}$  NMR (100 MHz,  $\text{CDCl}_3$ )  $\delta$  188.4, 149.9, 148.0, 145.4, 137.6 (2C), 137.2, 130.1, 126.1, 124.3, 118.2, 115.6 (2C), 111.8, 101.3, 55.8; HRMS (ESI-TOF) calcd for  $\text{C}_{16}\text{H}_{14}\text{IO}_3$  [ $\text{M} + \text{H}$ ] $^+$  380.99822, found 380.99852; mp 134–136  $^\circ\text{C}$ ; IR (Neat) 3341, 1644, 1572, 1549, 1515, 1233, 1209, 1058, 1026, 1004, 817, 738  $\text{cm}^{-1}$ ; HPLC  $t_{\text{R}}$  = 5.61 min, purity > 97% (254 nm).

**3-(2-Azidoethoxy)-4-(methoxymethoxy)benzaldehyde (39).** Step 1—Coupling with PEG chain: NaH (817 mg, 20.4 mmol, 60% w/w in oil) was suspended in anhydrous toluene (10 mL). Magnetic stirring was stopped after 5 min. After decantation, toluene was removed. Anhydrous DMSO (28 mL) and 3,4-dihydroxybenzaldehyde (1.69 g, 12.2 mmol) were added, and the mixture was allowed to warm at 25  $^\circ\text{C}$  for 1 h. 2-Azidoethyl 4-methylbenzenesulfonate (2.47 g, 10.2 mmol) in anhydrous DMSO (5 mL) was added slowly, and the mixture was stirred overnight at rt. The reaction was poured into 100 mL of ice–water and neutralized with 1 M aqueous HCl. The mixture was extracted 3 times with EtOAc. The combined organic layers were washed with brine, dried over anhydrous  $\text{Na}_2\text{SO}_4$ , filtered, and concentrated. Purification on silica gel eluting with 5–100% MeCN adding 0.1% TFA in water and freeze drying afforded 3-(2-azidoethoxy)-4-hydroxybenzaldehyde as a white powder (1.54 g, 7.43 mmol, 68%).  $^1\text{H}$  NMR (400 MHz,  $\text{CDCl}_3$ )  $\delta$  9.80 (s, 1H), 7.45 (d,  $J$  = 8.1 Hz, 1H), 7.41 (s, 1H), 7.06 (d,  $J$  = 8.1 Hz, 1H), 6.32 (br s, 1H), 4.29 (t,  $J$  = 4.9 Hz, 2H), 3.68 (t,  $J$  = 4.9 Hz, 2H);  $^{13}\text{C}$  NMR (100 MHz,  $\text{CDCl}_3$ )  $\delta$  190.8, 152.0, 145.9, 129.8, 128.2, 115.2, 110.5, 68.2, 50.1.

Step 2—Protection with MOMCl: To a solution of 3-(2-azidoethoxy)-4-hydroxybenzaldehyde (1.45 g, 7.00 mmol) in anhydrous acetone (6 mL) was added  $\text{K}_2\text{CO}_3$  (1.93 g, 14.0 mmol) and methoxymethyl chloride (797  $\mu\text{L}$ , 10.5 mmol). The mixture was allowed to stir at rt overnight. After removal of the solvent, water was added and the mixture was extracted 3 times with EtOAc. The combined organic layers were washed with brine, dried over anhydrous  $\text{Na}_2\text{SO}_4$ , filtered, and concentrated to obtain the desired compound as a white powder (1.67 g, 6.65 mmol, 95%).  $^1\text{H}$  NMR (400 MHz,  $\text{CDCl}_3$ )  $\delta$  9.82 (s, 1H), 7.43 (dd,  $J$  = 8.2 Hz, 2.0 Hz, 1H), 7.40 (d,  $J$  = 1.8 Hz, 1H), 7.22 (d,  $J$  = 1.8 Hz, 1H), 5.26 (s, 2H), 4.23 (t,  $J$  = 4.9 Hz, 2H), 3.62 (t,  $J$  = 4.9 Hz, 2H), 3.48 (s, 3H);  $^{13}\text{C}$  NMR (100 MHz,  $\text{CDCl}_3$ )  $\delta$  190.8, 152.5, 149.0, 131.0, 127.0, 115.4, 111.6, 94.9, 68.1, 56.6, 50.1.

**(E)-3-(3-(2-Azidoethoxy)-4-(methoxymethoxy)phenyl)-1-(4-chlorophenyl)prop-2-en-1-one (42).** To a solution of 3-(2-azidoethoxy)-4-(methoxymethoxy)benzaldehyde 39 (0.126 g, 0.50 mmol) were added 1-(4-chlorophenyl)propan-1-one (72  $\mu\text{L}$ , 0.55 mmol) and barium hydroxide monohydrate (189 mg, 1.00 mmol). After 4 h, the mixture was concentrated under vacuum. Water was added, and the aqueous layer was extracted 3 times with  $\text{CH}_2\text{Cl}_2$ . The combined organic layers were washed with brine, dried over

anhydrous  $\text{Na}_2\text{SO}_4$ , filtered, and concentrated to obtain the desired compound as a yellow powder (109 mg, 0.28 mmol, 56%).  $^1\text{H}$  NMR (400 MHz,  $\text{CDCl}_3$ )  $\delta$  7.67 (d,  $J$  = 8.6 Hz, 2H), 7.41 (d,  $J$  = 15.5 Hz, 1H), 7.18 (d,  $J$  = 8.6 Hz, 2H), 7.15 (d,  $J$  = 15.5 Hz, 1H), 7.00 (d,  $J$  = 1.9 Hz, 1H), 6.97 (dd,  $J$  = 8.4, 1.9 Hz, 1H), 6.85 (d,  $J$  = 8.4 Hz, 1H), 4.94 (s, 2H), 3.96 (t,  $J$  = 4.9 Hz, 2H), 3.34 (t,  $J$  = 4.9 Hz, 2H), 3.19 (s, 3H);  $^{13}\text{C}$  NMR (100 MHz,  $\text{CDCl}_3$ )  $\delta$  190.7, 150.3, 149.6, 146.2, 146.1, 130.6, 129.5, 124.6, 120.8, 117.3, 114.6, 95.8, 76.3, 69.2, 56.8, 50.9, 50.1.

**(E)-3-(3-(2-Aminoethoxy)-4-hydroxyphenyl)-1-(4-chlorophenyl)prop-2-en-1-one hydrochloride (45).** Step 1—Deprotection according to general procedure C using (E)-3-(3-(2-azidoethoxy)-4-(methoxymethoxy)phenyl)-1-(4-chlorophenyl)prop-2-en-1-one 42 (162 mg, 0.42 mmol). Yield of (E)-3-(3-(2-azidoethoxy)-4-hydroxyphenyl)-1-(4-chlorophenyl)prop-2-en-1-one was quantitative (162 mg, 0.42 mmol).  $^1\text{H}$  NMR (400 MHz,  $\text{MeOD}-d_4$ )  $\delta$  8.08 (d,  $J$  = 8.5 Hz, 2H), 7.76 (d,  $J$  = 15.6 Hz, 1H), 7.61 (d,  $J$  = 15.6 Hz, 1H), 7.56 (d,  $J$  = 8.5 Hz, 2H), 7.44 (d,  $J$  = 2.0 Hz, 1H), 7.35 (dd,  $J$  = 8.3, 2.0 Hz, 1H), 6.94 (d,  $J$  = 8.3 Hz, 1H), 4.35 (t,  $J$  = 4.9 Hz, 2H), 3.42 (t,  $J$  = 4.9 Hz, 2H);  $^{13}\text{C}$  NMR (100 MHz,  $\text{CDCl}_3$ )  $\delta$  191.1, 151.1, 147.8, 147.1, 140.4, 138.3, 131.4, 130.2, 128.8, 126.0, 120.3, 117.3, 114.8, 66.6, 40.6; MS  $m/z$  344.1 [ $\text{M} + \text{H}$ ] $^+$ .

Step 2—To a solution of (E)-3-(3-(2-azidoethoxy)-4-hydroxyphenyl)-1-(4-chlorophenyl)prop-2-en-1-one (10.0 mg, 0.03 mmol) in distilled water (0.77 mL) and THF (1.18 mL) was added polymer-supported triphenylphosphine (29 mg, 0.04 mmol). The mixture was allowed to stir overnight at rt. The reaction was then filtered, evaporated, purified on semipreparative HPLC (5–70% MeCN in water), treated with an aqueous solution of HCl 1 M, and freeze dried to afford the title compound (5 mg, 0.02 mmol, 55%) as a yellow powder.  $^1\text{H}$  NMR (400 MHz,  $\text{MeOD}-d_4$ )  $\delta$  8.08 (d,  $J$  = 8.6 Hz, 2H), 7.76 (d,  $J$  = 15.5 Hz, 1H), 7.61 (d,  $J$  = 15.5 Hz, 1H), 7.56 (d,  $J$  = 8.5 Hz, 2H), 7.44 (d,  $J$  = 2.0 Hz, 1H), 7.35 (dd,  $J$  = 8.4 Hz,  $J$  = 2.0 Hz, 1H), 6.94 (d,  $J$  = 8.3 Hz, 1H), 4.35 (t,  $J$  = 4.9 Hz, 2H), 3.43 (t,  $J$  = 4.9 Hz, 2H);  $^{13}\text{C}$  NMR (100 MHz,  $\text{MeOD}-d_4$ )  $\delta$  191.1, 151.1, 147.8, 147.1, 140.4, 138.2 (2C), 131.4, 130.2, 128.7, 126.0, 120.3, 117.3 (2C), 114.9, 66.6, 40.6; HRMS (ESI-TOF) calcd for  $\text{C}_{17}\text{H}_{17}\text{ClNO}_3$  [ $\text{M} + \text{H}$ ] $^+$  318.08915, found 318.08971; mp 260–262  $^\circ\text{C}$ ; IR (Neat) 3346, 3017, 1630, 1591, 1519, 1484, 1440, 1277, 1160, 1015, 975, 813, 614  $\text{cm}^{-1}$ ; HPLC  $t_{\text{R}}$  = 3.90 min, purity > 98% (254 nm).

**4-(3-(4-Chlorophenyl)-4,5-dihydro-1H-pyrazol-5-yl)-2-methoxyphenol (50).** To a solution of (E)-1-(4-chlorophenyl)-3-(4-hydroxy-3-methoxyphenyl)prop-2-en-1-one 1 (524 mg, 1.81 mmol, 1 equiv) in EtOH (2.6 mL) was added hydrazine monohydrate (265  $\mu\text{L}$ , 5.44 mmol). The reaction was allowed to reflux for 4 h. The mixture was then evaporated under reduced pressure and solubilized in EtOH (2.5 mL). Precipitation from *n*-heptane, centrifugation, and drying in vacuo afforded the desired compound as a white powder (457 mg, 1.51 mmol, 83%).  $^1\text{H}$  NMR (400 MHz,  $\text{MeOD}-d_4$ )  $\delta$  8.84 (br s, 1H), 7.64–7.59 (m, 2H), 7.57 (d,  $J$  = 3.2 Hz, 1H), 7.45–7.39 (m, 2H), 6.95 (d,  $J$  = 1.5 Hz, 1H), 6.79–6.70 (m, 2H), 4.76 (td,  $J$  = 10.9, 3.2 Hz, 1H), 3.75 (s, 3H), 3.42–3.29 (m, 1H), 2.82 (dd,  $J$  = 16.3 Hz, 11.0 Hz, 1H);  $^{13}\text{C}$  NMR (100 MHz,  $\text{MeOD}-d_4$ )  $\delta$  147.5, 147.4, 145.7 (2C), 133.4, 132.3, 132.2, 128.4, 126.9, 118.9, 115.2 (2C), 110.8, 63.8, 55.5, 42.3; HRMS (ESI-TOF) calcd for  $\text{C}_{16}\text{H}_{16}\text{ClN}_2\text{O}_2$  [ $\text{M} + \text{H}$ ] $^+$  303.09003, found 303.08959; mp 128–130  $^\circ\text{C}$ ; IR (Neat) 3358, 1582, 1518, 1336, 1269, 1234, 1206, 1029, 827, 813, 528  $\text{cm}^{-1}$ ; HPLC  $t_{\text{R}}$  = 3.86 min, purity > 97% (254 nm).

**4-(4-Chlorophenyl)-6-(4-hydroxy-3-methoxyphenyl)pyrimidin-2(1H)-one (57).** To a solution of (E)-1-(4-chlorophenyl)-3-(4-hydroxy-3-methoxyphenyl)prop-2-en-1-one 1 (100 mg, 0.34 mmol, 1 equiv) in EtOH (1.240 mL) were added urea (204 mg, 3.40 mmol, 10 equiv) and HCl in dioxane (840  $\mu\text{L}$ , 4 M). The mixture was allowed to reflux for 2 h. The reaction was then concentrated, and the residue was purified on a silica gel column eluting with 0–10% MeOH in  $\text{CH}_2\text{Cl}_2$  to afford after freeze drying an orange powder (48 mg, 0.15 mmol, 43%).  $^1\text{H}$  NMR (400 MHz,  $\text{DMSO}-d_6$ )  $\delta$  11.41 (br s, 1H), 10.24 (br s, 1H), 8.18 (d,  $J$  = 8.7 Hz, 2H), 7.78–7.69 (m, 2H), 7.64 (d,  $J$  = 8.7 Hz, 2H), 7.51 (s, 1H), 6.99 (d,  $J$  = 8.2 Hz, 1H), 3.90 (s, 3H);  $^{13}\text{C}$  NMR (100 MHz,  $\text{DMSO}-d_6$ )  $\delta$  163.7, 163.1, 156.6,



151.6, 147.9 (2C), 136.9, 132.6, 129.8, 128.9, 122.9, 122.6, 115.7 (2C), 111.5, 99.2, 55.9; HRMS (ESI-TOF) calcd for  $C_{17}H_{14}ClN_2O_3$   $[M + H]^+$  329.06875, found 329.06876; mp 306–308 °C; IR (Neat) 3464, 1728, 1666, 1590, 1310, 1262, 1216, 1153, 1089, 795, 774, 622, 490  $cm^{-1}$ ; HPLC  $t_R$  = 3.46 min, purity > 97% (254 nm).

**(E)-7-Chloro-3-(4-hydroxy-3-methoxybenzylidene)chroman-4-one (65).** To a solution 7-chlorochroman-4-one (156 mg, 0.86 mmol) and 4-hydroxy-3-methoxybenzaldehyde (131 mg 0.86 mmol) in EtOH (1.80 mL),  $SOCl_2$  (88  $\mu L$ , 1.00 mmol) was added dropwise at rt. The reaction mixture was stirred for 5 h. The solvent was then evaporated in vacuo, and the crude product was recrystallized from EtOH affording the desired compound (145 mg, 0.46 mmol, 53%) as a yellow solid.  $^1H$  NMR (400 MHz,  $CDCl_3$ )  $\delta$  7.93 (d,  $J$  = 8.5 Hz, 1H), 7.79 (t,  $J$  = 1.9 Hz, 1H), 7.02 (dd,  $J$  = 8.5, 2.0 Hz, 1H), 6.98 (d,  $J$  = 7.8 Hz, 1H), 6.97 (d,  $J$  = 2.0 Hz, 1H), 6.82 (d,  $J$  = 2.0 Hz, 1H), 6.81 (dd,  $J$  = 7.8, 2.0 Hz, 1H), 5.92 (s, 1H), 5.37 (d,  $J$  = 1.9 Hz, 2H), 3.91 (s, 3H);  $^{13}C$  NMR (100 MHz,  $CDCl_3$ )  $\delta$  181.4, 161.5, 147.7, 146.8, 141.7, 138.5, 129.3, 128.4, 126.9, 124.5, 122.8, 120.8, 118.2, 115.0, 113.1, 68.4, 56.2; HRMS (ESI-TOF) calcd for  $C_{17}H_{14}ClO_4$   $[M + H]^+$  317.0575, found 317.0583; mp 180–182 °C; IR (Neat) 3502, 1658, 1567, 1512, 1444, 1261, 1206, 1127, 1027, 842, 805, 490  $cm^{-1}$ ; HPLC  $t_R$  = 5.70 min, purity > 97% (254 nm).

**(E)-1-(4-Chloro-2-hydroxyphenyl)-3-(3-methoxy-4-(methoxymethoxy)phenyl)prop-2-en-1-one (66).** To a solution of 3-methoxy-4-(methoxymethoxy)benzaldehyde (180 mg, 0.92 mmol) in EtOH (2.5 mL) were added 1-(4-chloro-2-hydroxyphenyl)ethan-1-one (234 mg, 1.34 mmol) and  $Ba(OH)_2 \cdot H_2O$  (157 mg, 0.83 mmol). The reaction was stirred for 48 h at rt. The mixture was evaporated. Purification on flash chromatography eluting with 5–100% EtOAc in *n*-heptane afforded the desired product (100 mg, 0.29 mmol, 28%). The corresponding product was directly engaged in the next step without analysis.

**(Z)-6-Chloro-2-(4-hydroxy-3-methoxybenzylidene)benzofuran-3(2H)-one (67).** **(E)-1-(4-Chloro-2-hydroxyphenyl)-3-(3-methoxy-4-(methoxymethoxy)phenyl)prop-2-en-1-one 66** (40 mg, 0.11 mmol) was added to 0.1 M  $Hg(AcO)_2$  in anhydrous pyridine (1.14 mL). The mixture was stirred for 1 h at 110 °C. After cooling it was poured into ice/water (100 mL) and acidified with 1 M aqueous HCl. The precipitate was recovered, dissolved with  $CH_2Cl_2$  (5 mL), and washed once with water and then with brine. The organic layer was dried over anhydrous  $Na_2SO_4$ , and the solvent was evaporated in vacuo. The crude was purified by flash chromatography on a silica gel column eluting with 10–50% EtOAc in *n*-heptane affording 12 mg (0.029 mmol, 25%) of protected compound. The title compound was obtained after deprotection according to general procedure C (quantitative yield).  $^1H$  NMR (400 MHz,  $CDCl_3$ )  $\delta$  9.92 (br s, 1H), 7.86–7.76 (m, 2H), 7.62 (s, 1H), 7.51 (br d,  $J$  = 8.2 Hz, 1H), 7.36 (br d,  $J$  = 8.1 Hz, 1H), 6.95 (s, 1H), 6.91 (br d,  $J$  = 8.2 Hz, 1H), 3.86 (s, 3H);  $^{13}C$  NMR (100 MHz,  $CDCl_3$ )  $\delta$  181.7, 165.1, 149.7, 147.8, 144.9, 141.1, 126.3, 125.3, 124.2, 122.9, 120.3, 116.0, 115.2, 114.5, 113.8, 55.6; HRMS (ESI-TOF) calcd for  $C_{16}H_{12}ClO_4$   $[M + H]^+$  303.04241, found 303.04182; mp 206–208 °C; IR (Neat) 3545, 1696, 1646, 1600, 1582, 1518, 1307, 1267, 1201, 1137, 1125, 1057, 1032, 841, 764  $cm^{-1}$ ; HPLC  $t_R$  = 5.42 min, purity > 98% (254 nm).

**Physicochemical Properties.** Solubility and stability studies were performed using a Gilson HPLC system with a photodiode array detector for analyses. Data acquisition and processing were performed with Trilution LC V2.0 software. Measurements were carried out at room temperature. A 5  $\mu m$  Luna C18(2) (50  $\times$  4.6 mm) purchased from Phenomenex was used. The mobile phase flow rate was 2 mL/min, and the following program was applied for the elution: 0–0.7 min, 0% B; 0.7–3.2 min, 0–100% B; 3.2–3.7 min, 100% B; 3.7–3.9 min, 100–0% B and 3.9–6.7 min, 0% B. Solvent B was HPLC-grade acetonitrile (Sigma-Aldrich CHROMASOLV). The aqueous solvent contained 0.01% trifluoroacetic acid. The detection wavelengths were 280 and 365 nm.

**Solubility.** Kinetic solubility was measured for all of the compounds in a pH 7.4 HEPES-BSA buffer with the following composition: NaCl 137.5 mM,  $MgCl_2$  1.25 mM,  $CaCl_2$  1.25 mM, KCl 6 mM, glucose 5.6 mM,  $NaH_2PO_4$  0.4 mM, HEPES 10 mM, and 1 g/L bovine serum

albumin. This method mimicked the conditions of the FRET-based binding experiments. Every compound was initially predissolved in DMSO at 10 mM. An aliquot of the DMSO solution was added to the buffer to reach a 5  $\mu M$  concentration. Samples were shaken during 24 h at 20 °C. After centrifugation, the concentration in the supernatant was measured by a HPLC procedure using two standard solutions (5 and 10  $\mu M$ ).

Thermodynamic solubility was measured for seven selected compounds by dissolving powders until saturation in pH 7.4 PBS (phosphate-buffered saline containing 100 mM sodium phosphate and 150 mM sodium chloride). Samples were shaken during 24 h at 20 °C. After centrifugation, the concentration in the supernatant was measured by a HPLC procedure using a calibration line established for each compound by diluting the 10 mM DMSO stock solution to adapted concentrations.

**Chemical Stability.** The stability of the same seven compounds selected for the thermodynamic solubility study was assessed in PBS pH 7.4 or PBS/Cdx (10% w/w) at 20 °C for up to 24 h. For each compound the stock solution was diluted to a final incubation concentration of 10  $\mu M$  with 1% DMSO. A 50  $\mu L$  amount of sample was removed at  $t_0$ , 2, 4, 6, and 24 h and directly injected onto the HPLC. The percentage of remaining test compound relative to  $t_0$  was measured by monitoring the peak area of the chromatogram.

**Michael Addition.** Michael acceptor reactivity was evaluated by incubating the compounds with reduced glutathione (GSH). Incubation mixtures contained 250  $\mu L$  of methanol, 500  $\mu M$  GSH (25  $\mu L$  of a 10 mM GSH solution), 200  $\mu M$  compound (10  $\mu L$  of the 10 mM DMSO stock solution), and 215  $\mu L$  of a 50 mM carbonate buffer adjusted at pH 8 (final volume of 500  $\mu L$ ). Five microliter aliquots of the reaction mixture were removed after 1 min and 2 h incubation. Samples were diluted 1/40 in water 0.05% formic acid/acetonitrile 1/1 and analyzed by LC-MS/MS for GSH-conjugate formation.

**Computational Methods.** Starting from the X-ray structure of the CXCL12 bound to inhibitor 3GG (PDB ID 4UAI), all nonprotein atoms (inhibitor, sulfate ions, water molecules) were removed and hydrogens added with Protoss v2.1<sup>41</sup> while optimizing protonation, ionization, and tautomeric states of all protein atoms. A 2D sketch of compound 1 was converted into a 2D MOL2 file with Corina v3.40 (Molecular Networks GmbH, Erlangen, Germany). The crystal structure of compound 57 (Figure S1) was converted into a MOL2 file format and used as such for docking with PLANTS v1.2.<sup>36</sup> The binding site was defined as a 12 Å radius sphere centered on the center of mass of the Trp57 cavity, deduced from the VolSite software.<sup>35</sup> Three side chains (Arg20, Trp57, and Tyr61) were allowed to freely move during the docking, performed with the speed1 search speed and the chemplp scoring function. For Surflex-Dock v3.066<sup>37</sup> a “protomol” was first generated using a list of binding site residues encompassing the above-described 12 Å sphere. The protein residues side chains were kept rigid, except for Arg20, Trp57, and Tyr61, which were considered fully flexible. Other parameters were assigned as default. The docking accuracy parameter set—pgeom was used.

**Biological Evaluation. Generation of HEK-293 Cells Stably Expressing Human CXCR4 Chemokine Receptor.** Human cDNA encoding CXCR4 receptor was cloned in pCEP4 vector (Life Technologies). The receptor is cloned in frame with a signal peptide fused to enhanced green fluorescent protein (EGFP) as described previously. The open reading frame was fully sequenced prior to transfection. Human Embryonic Kidney HEK-293 cells were obtained from ATCC and maintained in minimal essential medium (MEM) (Invitrogen) supplemented with 10% fetal bovine serum (FBS) (Gibco-BRL), 100 U/mL penicillin (Invitrogen), 100  $\mu g/mL$  streptomycin (Invitrogen), and 2 mM L-glutamine (Invitrogen) at 37 °C in an atmosphere of 95% air and 5%  $CO_2$ . HEK-293 cells were transfected with 15  $\mu g$  of the human CXCR4 chemokine receptor in pCEP4 plasmid using a calcium phosphate precipitation method in 10 cm dishes. Stably EGFP-CXCR4-expressing HEK cells were selected by addition of hygromycin (Life technologies) for 5 weeks. The

resulting cell clones were checked by fluorescence microscopy and fluorescence-activated cell sorting (FACS) analysis.

**FRET-Based Binding Assay.** HEK EGFP-CXCR4-expressing cells were washed with phosphate-buffered saline (PBS) and detached in PBS-ethylene diamine tetra-acetic acid (EDTA, 5 mM) (Sigma-Aldrich) for 2 min at room temperature. Then cells were carefully resuspended in complete growth medium, pelleted by centrifugation at  $320 \times g$  for 5 min, and resuspended in HEPES buffer (137.5 mM NaCl, 6 mM KCl, 1.25 mM  $\text{CaCl}_2$ , 1.25 mM  $\text{MgCl}_2$ , 0.4 mM  $\text{NaH}_2\text{PO}_4$ , 5.6 mM glucose, 10 mM HEPES (4-(2-hydroxyethyl)-1-piperazineethanesulfonic acid), pH 7.4) containing 0.1% bovine serum albumin (w/v) (BSA) (all from Sigma-Aldrich). Cells were used at a concentration of  $10^6$  cells/mL,<sup>34</sup> then the cell suspension (1 mL) was transferred into a quartz cuvette. Time-based recordings of the fluorescence emitted at 510 nm (excitation at 470 nm) were performed at 21 °C using a Fluorolog 3 spectrofluorometer (JobinYvon/Spex). Fluorescence binding measurements were initiated by adding at  $t = 150$  s, 100 nM CXCL12-Texas Red (TR) (Almac) to the 1 mL cell suspension. Binding of CXCL12-TR to EGFP-labeled CXCR4 was detected as a reversible decline of emission at 510 nm due to energy transfer from excited EGFP to TR. In the “neutraligand protocol”, CXCL12-TR was preincubated for 1 h at room temperature with DMSO or various concentrations of each test compound. Then the premix was added (at  $t = 150$  s), and fluorescence was recorded until equilibrium was reached (300 s). In the “antagonist protocol”, DMSO or various concentrations of each test compound were added to EGFP-CXCR4-expressing cells at  $t = 50$  s. Then CXCL12-Texas Red (100 nM) was added at  $t = 150$  s, and fluorescence was recorded until equilibrium was reached (300 s). Dose–response curves of inhibition of CXCL12-TR binding were performed, and the inhibitory constants ( $K_i$ ) of the different compounds were determined. T134 (20  $\mu\text{M}$ ), the CXCR4 receptor antagonist, was used as a control in both “neutraligand” and “antagonist” protocols. Data were analyzed using Kaleidagraph 4.1.3 software (Synergy Software, Reading, PA).

**Allergic Eosinophilic Airway Inflammation Mouse Model.** The activity of each compound was assessed in vivo in an 8 day model of allergic eosinophilic airway inflammation as described previously.<sup>21,33</sup> Briefly, 9 week-old male Balb/c mice were sensitized by intraperitoneal injection of 50  $\mu\text{g}$  of ovalbumin (OVA, grade V, Sigma-Aldrich, A5503) adsorbed on 2 mg of aluminum hydroxide (Sigma-Aldrich, 23918–6) in 0.1 mL of saline on days 0, 1, and 2. Mice were challenged intranasally [10  $\mu\text{g}$  of OVA in 25  $\mu\text{L}$  of saline (12.5  $\mu\text{L}$ /nostril)] on days 5, 6, and 7. Control mice received intranasal administration of saline alone. Intranasal administrations were performed under anesthesia with intraperitoneal injection of ketamine (50 mg/kg) and xylazine (3.33 mg/kg). Food and water were supplied ad libitum. Animal experimentation was conducted with the approval of the agriculture ministry regulating animal research in France (Ethics regional committee for animal experimentation-Strasbourg, APAFIS 1341#2015080309399690). Two hours before each OVA or saline challenge, compounds in PBS/Cdx were administered intranasally (12.5  $\mu\text{L}$ /nostril), intraperitoneally, or per os as indicated in the figure legends. Bronchoalveolar lavage (BAL) was performed 24 h after the last OVA or saline challenge as described.<sup>34</sup> Mice were deeply anesthetized by intraperitoneal injection of ketamine (Imalgene, 150 mg/kg) and xylazine (Rompun, 10 mg/kg). A plastic cannula was inserted into the trachea, and airways were lavaged by 10 instillations of 0.5 mL of ice-cold saline supplemented with 2.6 mM EDTA (saline-EDTA). BAL fluids were centrifuged (300g, 5 min, 4 °C) to pellet cells, and erythrocytes were lysed by hypotonic shock. Cells were resuspended in 500  $\mu\text{L}$  of ice-cold saline-EDTA, and total cell counts were determined on a hemocytometer (Neubauer, PRECIS). Differential cell counts were assessed on cytological preparations (Cytospin 4, Thermo Fischer Scientific) spanning 250 000 cells/mL in ice-cold saline–EDTA, stained with Diff-Quick (Merck, 111674) with counts of at least 400 cells. Counts were expressed as absolute cell numbers or percentage of inhibition of eosinophil recruitment. The differential number of cells in BALF and the eosinophil inhibition (%) are presented as means  $\pm$

SEM. Differences between groups were tested for statistical significance using a one-way ANOVA followed by Tukey post-test. Data were considered significantly different when the  $p$  value is  $<0.05$ .

## ■ ASSOCIATED CONTENT

### ⑤ Supporting Information

The Supporting Information is available free of charge on the ACS Publications website at DOI: 10.1021/acs.jmedchem.8b00657.

General procedures and experimental data for compounds 2–21, 23–28, 30–38, 40, 41, 43, 44, 46–49, 51–56, 58–64, and 68; crystallographic structure for 1 and 57 (CCDC 1578824–1578825), and chemical stability study of 1 and 57 toward reduced glutathione; molecular formula strings (PDF) (CSV)

## ■ AUTHOR INFORMATION

### Corresponding Authors

\*E-mail: nelly.frossard@unistra.fr.

\*E-mail: dominique.bonnet@unistra.fr.

### ORCID

Marcel Hibert: 0000-0001-7786-7276

Dominique Bonnet: 0000-0002-8252-9199

### Notes

The authors declare no competing financial interest.

## ■ ACKNOWLEDGMENTS

This work was supported by the Agence Nationale de la Recherche (ANR-07-PCVI-0026-02), the Centre National de la Recherche Scientifique, the Université de Strasbourg, and the LABEX Medalis (ANR-10-LABX-0034). P.R. was supported by a fellowship from the Ministère de l'Éducation Nationale, de l'Enseignement Supérieur et de la Recherche. F.D. was the recipient of fellowships from the Fonds de recherche en santé respiratoire (FRSR) and Région Alsace. D.A. was a fellow of the CNRS and of Greenpharma SA. We are grateful to Cyril Antheaume, Barbara Schaeffer, and Justine Vieville for NMR experiments, to Pascale Buisine and Patrick Wehrung for mass spectrometry (PACSI platform GDS3670), and to Lydia Karmazin for crystallographic structures (Service de Radiocristallographie, Platform GDS 3648, Strasbourg).

## ■ ABBREVIATIONS USED

BAL, bronchoalveolar lavage; BSA, bovine serum albumin; Cdx, 2-hydroxypropyl- $\beta$ -cyclodextrin; CXCL12, C-X-C chemokine 12; CXCR4, C-X-C chemokine receptor type 4; G6P, glucose-6-phosphate; G6PDH, glucose-6-phosphate dehydrogenase; HEPES, 4-(2-hydroxyethyl)-1-piperazineethanesulfonic acid; HIV, human immunodeficiency virus; i.n., intranasal; LC-MS, liquid chromatography-mass spectrometry; MOM, methoxymethyl; NADP, nicotinamide adenine dinucleotide phosphate; OVA, ovalbumin; PBS, phosphate-buffered saline; PS, polymer supported; RP-HPLC, reversed-phase high-performance liquid chromatography; SAR, structure–activity relationship; SEM, standard error of the mean; TBDMS, *tert*-butyldimethylsilyl; TCEP, tris (2-carboxyethyl) phosphine; TR, Texas red; WHIM, warts, hypogammaglobulinemia, infections, and myelokathexis



## REFERENCES

- (1) Zou, Y.-R.; Kottmann, A. H.; Kuroda, M.; Taniuchi, I.; Littman, D. R. Function of the chemokine receptor CXCR4 in hematopoiesis and in cerebellar development. *Nature* **1998**, *393*, 595–599.
- (2) Tran, P. B.; Miller, R. J. Chemokine receptors: signposts to brain development and disease. *Nat. Rev. Neurosci.* **2003**, *4*, 444–455.
- (3) Fernandez, E. J.; Lolis, E. Structure, function, and inhibition of chemokines. *Annu. Rev. Pharmacol. Toxicol.* **2002**, *42*, 469–499.
- (4) Mantovani, A. The chemokine system: redundancy for robust outputs. *Immunol. Today* **1999**, *20*, 254–257.
- (5) Johnson, Z.; Schwarz, M.; Power, C. A.; Wells, T. N. C.; Proudfoot, A. E. I. Multi-faceted strategies to combat disease by interference with the chemokine system. *Trends Immunol.* **2005**, *26*, 268–274.
- (6) Moser, B.; Willmann, K. Chemokines: role in inflammation and immune surveillance. *Ann. Rheum. Dis.* **2004**, *63*, ii84–ii89.
- (7) Godessart, N.; Kunkel, S. L. Chemokines in autoimmune disease. *Curr. Opin. Immunol.* **2001**, *13*, 670–675.
- (8) Lazennec, G.; Richmond, A. Chemokines and chemokine receptors: new insights into cancer-related inflammation. *Trends Mol. Med.* **2010**, *16*, 133–144.
- (9) Balkwill, F. R. The chemokine system and cancer. *J. Pathol.* **2012**, *226*, 148–157.
- (10) Koenen, R. R.; Weber, C. Therapeutic targeting of chemokine interactions in atherosclerosis. *Nat. Rev. Drug Discovery* **2010**, *9*, 141–153.
- (11) Brauersreuther, V.; Mach, F.; Steffens, S. The specific role of chemokines in atherosclerosis. *Thromb. Haemostasis* **2007**, *97*, 714–721.
- (12) Wenzel, J.; Henze, S.; Worenkamper, E.; Basner-Tschakarjan, E.; Sokolowska-Wojdylo, M.; Steitz, J.; Bieber, T.; Tuting, T. Role of the chemokine receptor CCR4 and its ligand thymus- and activation-regulated chemokine/CCL17 for lymphocyte recruitment in cutaneous lupus erythematosus. *J. Invest. Dermatol.* **2005**, *124*, 1241–1248.
- (13) Bendall, L. Chemokines and their receptors in disease. *Histol. Histopathol.* **2005**, *20*, 907–926.
- (14) Zipp, F.; Hartung, H. P.; Hillert, J.; Schimrigk, S.; Trebst, C.; Stangel, M.; Infante-Duarte, C.; Jakobs, P.; Wolf, C.; Sandbrink, R.; Pohl, C.; Filippi, M. Blockade of chemokine signaling in patients with multiple sclerosis. *Neurology* **2006**, *67*, 1880–1883.
- (15) Brown, M. F.; Bahnck, K. B.; Blumberg, L. C.; Brissette, W. H.; Burrell, S. A.; Driscoll, J. P.; Fedeles, F.; Fisher, M. B.; Foti, R. S.; Gladue, R. P.; Guzman-Martinez, A.; Hayward, M. M.; Lira, P. D.; Lillie, B. M.; Lu, Y.; Lundquist, G. D.; McElroy, E. B.; McGlynn, M. A.; Paradis, T. J.; Poss, C. S.; Roache, J. H.; Shavnya, A.; Shepard, R. M.; Trevena, K. A.; Tylaska, L. A. Piperazinyl CCR1 antagonists—optimization of human liver microsome stability. *Bioorg. Med. Chem. Lett.* **2007**, *17*, 3109–3112.
- (16) Johnson, M.; Li, A. R.; Liu, J.; Fu, Z.; Zhu, L.; Miao, S.; Wang, X.; Xu, Q.; Huang, A.; Marcus, A.; Xu, F.; Ebsworth, K.; Sablan, E.; Danao, J.; Kumer, J.; Dairaghi, D.; Lawrence, C.; Sullivan, T.; Tonn, G.; Schall, T.; Collins, T.; Medina, J. Discovery and optimization of a series of quinazolinone-derived antagonists of CXCR3. *Bioorg. Med. Chem. Lett.* **2007**, *17*, 3339–3343.
- (17) Horuk, R. Chemokine receptor antagonists: overcoming developmental hurdles. *Nat. Rev. Drug Discovery* **2009**, *8*, 23–33.
- (18) Hachet-Haas, M.; Balabanian, K.; Rohmer, F.; Pons, F.; Franchet, C.; Lecat, S.; Chow, K. Y.; Dagher, R.; Gizzi, P.; Didier, B.; Lagane, B.; Kellenberger, E.; Bonnet, D.; Baleux, F.; Haiech, J.; Parmentier, M.; Frossard, N.; Arenzana-Seisdedos, F.; Hibert, M.; Galzi, J. L. Small neutralizing molecules to inhibit actions of the chemokine CXCL12. *J. Biol. Chem.* **2008**, *283*, 23189–23199.
- (19) Balabanian, K.; Brotin, E.; Biajoux, V.; Bouchet-Delbos, L.; Lainey, E.; Fenneteau, O.; Bonnet, D.; Fiette, L.; Emilie, D.; Bachelier, F. Proper desensitization of CXCR4 is required for lymphocyte development and peripheral compartmentalization in mice. *Blood* **2012**, *119*, 5722–5730.
- (20) Romain, B.; Hachet-Haas, M.; Rohr, S.; Brigand, C.; Galzi, J. L.; Gaub, M. P.; Pencreach, E.; Guenot, D. Hypoxia differentially regulated CXCR4 and CXCR7 signaling in colon cancer. *Mol. Cancer* **2014**, *13*, 58.
- (21) Gasparik, V.; Daubeuf, F.; Hachet-Haas, M.; Rohmer, F.; Gizzi, P.; Haiech, J.; Galzi, J. L.; Hibert, M.; Bonnet, D.; Frossard, N. Prodrugs of a CXC Chemokine-12 (CXCL12) Neutraligand prevent inflammatory reactions in an asthma model in vivo. *ACS Med. Chem. Lett.* **2012**, *3*, 10–14.
- (22) Daubeuf, F.; Hachet-Haas, M.; Gizzi, P.; Gasparik, V.; Bonnet, D.; Utard, V.; Hibert, M.; Frossard, N.; Galzi, J. L. An antedrug of the CXCL12 neutraligand blocks experimental allergic asthma without systemic effect in mice. *J. Biol. Chem.* **2013**, *288*, 11865–11876.
- (23) Veldkamp, C. T.; Ziarek, J. J.; Peterson, F. C.; Chen, Y.; Volkman, B. F. Targeting SDF-1/CXCL12 with a ligand that prevents activation of CXCR4 through structure-based drug design. *J. Am. Chem. Soc.* **2010**, *132*, 7242–7243.
- (24) Smith, E. W.; Liu, Y.; Getschman, A. E.; Peterson, F. C.; Ziarek, J. J.; Li, R. S.; Volkman, B. F.; Chen, Y. Structural analysis of a novel small molecule ligand bound to the CXCL12 chemokine. *J. Med. Chem.* **2014**, *57*, 9693–9699.
- (25) Smith, E. W.; Nevins, A. M.; Qiao, Z.; Liu, Y.; Getschman, A. E.; Vankayala, S. L.; Kemp, M. T.; Peterson, F. C.; Li, R. S.; Volkman, B. F.; Chen, Y. Structure-based identification of novel ligands targeting multiple sites within a chemokine–G-protein-coupled-receptor interface. *J. Med. Chem.* **2016**, *59*, 4342–4351.
- (26) Weisberg, E. L.; Sattler, M.; Azab, A. K.; Eulberg, D.; Kruschinski, A.; Manley, P. W.; Stone, R.; Griffin, J. D. Inhibition of SDF-1-induced migration of oncogene-driven myeloid leukemia by the L-RNA aptamer (Spiegelmer), NOX-A12, and potentiation of tyrosine kinase inhibition. *Oncotarget* **2017**, *8*, 109973–109984.
- (27) Rucker, H.; Al-Rifai, N.; Rascle, A.; Gottfried, E.; Brodziak-Jaros, L.; Gerhauser, C.; Dick, T. P.; Amslinger, S. Enhancing the anti-inflammatory activity of chalcones by tuning the Michael acceptor site. *Org. Biomol. Chem.* **2015**, *13*, 3040–3047.
- (28) Chimenti, F.; Fioravanti, R.; Bolasco, A.; Manna, F.; Chimenti, P.; Secci, D.; Befani, O.; Turini, P.; Ortuso, F.; Alcaro, S. Monoamine oxidase isoform-dependent tautomeric influence in the recognition of 3,5-diaryl pyrazole inhibitors. *J. Med. Chem.* **2007**, *50*, 425–428.
- (29) Maillet, E. L.; Pellegrini, N.; Valant, C.; Bucher, B.; Hibert, M.; Bourguignon, J. J.; Galzi, J. L. A novel, conformation-specific allosteric inhibitor of the tachykinin NK2 receptor (NK2R) with functionally selective properties. *FASEB J.* **2007**, *21*, 2124–2134.
- (30) Valenzuela-Fernandez, A.; Palanche, T.; Amara, A.; Magerus, A.; Altmeyer, R.; Delaunay, T.; Virelizier, J. L.; Baleux, F.; Galzi, J. L.; Arenzana-Seisdedos, F. Optimal inhibition of X4 HIV isolates by the CXC chemokine stromal cell-derived factor 1 alpha requires interaction with cell surface heparan sulfate proteoglycans. *J. Biol. Chem.* **2001**, *276*, 26550–26558.
- (31) Galzi, J.-L.; Haas, M.; Frossard, N.; Hibert, M. Why and how to find neutraligands targeting chemokines? *Drug Discovery Today: Technol.* **2012**, *9*, e245–e251.
- (32) Gould, S.; Scott, R. C. 2-Hydroxypropyl-beta-cyclodextrin (HP-beta-CD): a toxicology review. *Food Chem. Toxicol.* **2005**, *43*, 1451–1459.
- (33) Daubeuf, F.; Frossard, N. Acute asthma models to ovalbumin in the mouse. *Curr. Protoc. Mouse Biol.* **2011**, *3*, 31–37.
- (34) Daubeuf, F.; Frossard, N. Performing bronchoalveolar lavage in the mouse. *Curr. Protoc. Mouse Biol.* **2012**, *2*, 167–175.
- (35) Desaphy, J.; Azdimousa, K.; Kellenberger, E.; Rognan, D. Comparison and druggability prediction of protein-ligand binding sites from pharmacophore-annotated cavity shapes. *J. Chem. Inf. Model.* **2012**, *52*, 2287–2299.
- (36) Korb, O.; Stutzle, T.; Exner, T. E. Empirical scoring functions for advanced protein-ligand docking with PLANTS. *J. Chem. Inf. Model.* **2009**, *49*, 84–96.
- (37) Jain, A. N. Surflex-Dock 2.1: Robust performance from ligand energetic modeling, ring flexibility, and knowledge-based search. *J. Comput.-Aided Mol. Des.* **2007**, *21*, 281–306.

- (38) Schneider, N.; Lange, G.; Hindle, S.; Klein, R.; Rarey, M. A consistent description of HYdrogen bond and DEhydration energies in protein-ligand complexes: methods behind the HYDE scoring function. *J. Comput.-Aided Mol. Des.* **2013**, *27*, 15–29.
- (39) Abboud, D.; Daubeuf, F.; Do, Q. T.; Utard, V.; Villa, P.; Haiech, J.; Bonnet, D.; Hibert, M.; Bernard, P.; Galzi, J. L.; Frossard, N. A strategy to discover decoy chemokine ligands with an anti-inflammatory activity. *Sci. Rep.* **2015**, *5*, 2045–2322.
- (40) Lukacs, N. W.; Berlin, A.; Schols, D.; Skerlj, R. T.; Bridger, G. J. AMD3100, a CXCR4 antagonist, attenuates allergic lung inflammation and airway hyperreactivity. *Am. J. Pathol.* **2002**, *160*, 1353–1360.
- (41) Bietz, S.; Urbaczek, S.; Schulz, B.; Rarey, M. Protoss: a holistic approach to predict tautomers and protonation states in protein-ligand complexes. *J. Cheminf.* **2014**, *6*, 12.